

A way to establish a framework of Astrobiology

MARUYAMA, Shigenori^{1*} ; EBISUZAKI, Toshikazu² ; NAKAMURA, Eizo³

¹Earth-Life Science Institute, Tokyo Institute of Technology, ²RIKEN, ³Institute for study of the Earth's interior, Okayama University

One of an ultimate mysteries of Science is the existence of life in the Universe. In regard to this question, three ideas have been provided; (1) The Universe teems with life, (2) No other life other than Earth life, and (3) between 1 and 2. Also, we have two simple questions about life. (1) Is primitive life constantly emerging on present Earth? (2) Once whole life is killed, another new Earth life will emerge on the Earth? The answer to both questions is No.

Astrobiology is the academic field that can provide minimum conditions to bear life in the Universe, and also collateral conditions to make a planet to have civilization. Here we summarize such conditions to have life with civilization. To emerge life on the Earth, there are numerous kinds of conditions which are intricately interrelated. Here, we categorized such complex conditions into three groups. (1) Conditions to make life-sustainable planets derived from planetary formation theory. This category lists 19 conditions. For example, elliptical orbit is unacceptable condition for life. Even if such planet is covered by liquid water, planet is to experience snowball for half the year, and for other half year water component turn to vapor due to red hot scorching environment like Venus. (2) Conditions to emerge and evolve life on the planet. This category includes 7 significant conditions which control the emergence and evolution of life. One of conditions is lifetime of carbon. Carbon is necessary component for life body, however the amount of carbon for life is decreasing through time. Carbon will be depleted in 1 billion years, indicating termination of life. (3) Conditions to have civilization on the planet. This category has 5 conditions. The most significant condition is brain development. Discontinuous upgrowth of brain differentiate human being from chimpanzee, and human is to establish civilization finally.

Possible meteoritic materials in spherules discovered in the Oikeyama impact crater

SAKAMOTO, Masao^{1*} ; NINAGAWA, Kiyotaka² ; NISHIDO, Hirotsugu³ ; GUCSIK, Arnold⁴

¹Iida City Museum, ²Okayama University of Science, ³Okayama University of Science, ⁴University of Johannesburg

Sakamoto et al. (2010) reported a first meteor crater in central Japan, where is located at the Mt. Oikeyama in Shirabiso highland, Iida City, Nagano Prefecture. It has been supported by the shocked quartz with planar deformation features (PDFs) and planar fractures (PFs) and a negative gravity anomaly around the crater (Sakamoto and Shichi, 2011). Recently, large numbers of spherules were found out at around the Oikeyama crater site. In this study we have conducted to clarify the origin of the spherules by the optical examination and chemical analysis.

A topographic feature of the crater indicates about 900 m in diameter, whereas its half of the rim in the eastern side was collapsed away under geological conditions. A rip-up crust containing a large number of spherules was observed at the slope outside 400m far from the rim. Eighty-percent part of the rip-up crust is composed of the spherules and their fragments, and ten-percent part is occupied by neighboring rock fragments and mud as a matrix. Most spherules indicate an imperfect globular shape and translucent to opaque under a microscope. Pyrite commonly occurs in the crust associated with the spherules, where small particles of pyrite are found as an ingrown crystal into the spherule. A polarizing microscopy shows that the spherules contain recrystallized and cryptocrystalline materials with microlite texture. There were many types of spherules including aggregate structure incorporated with other small spherule and zoned texture with the core of opaque material and rim of translucent one.

We obtained chemical-compositional map of Mg, Si, S, V, Cr, Mn, Fe, Ni, and Ir in the spherules and associated fragments in the rip-up crust by the use of a laser ablation-inductively coupled plasma-mass spectrometry (LA-ICP-MS). The result indicates inhomogeneous distribution of such elements in and around the spherules. Relative high concentrations of Ni, V, Cr, Mg, Mn and Fe are observed, suggesting the same type of spherules in the Late Archaean Paraborhood impact crater reported by Izmer et al. (2013).

Oikeyama area geologically consists of sandstone, mudstone and chert belonging to Chichibu Paleozoic terrain, where the elements of Ni, V and Cr are not predominant in these sediments. Pyrite is not usually found in the volcanic-aeolian sediments in this area, although pyrite is frequently accompanied with the spherules in the rip-up crust.

References

Sakamoto et al. 2010, *Meteorit. & Planet. Sci.* 45; Sakamoto and Shichi 2010, *Japanese Society for Planetary Science* 19, 4; Izmer et al. 2013, *J. Anal. At. Spectrom.*, 28;

Keywords: Oikeyama Crater, impact, spherule, pyrite, nickel, meteoritic material

Weighted Particle Hydrodynamics without Riemann Solver

HOSONO, Natsuki^{1*}; MAKINO, Junichiro¹

¹RIKEN Advanced Institute for Computational Science, ²Earth-Life Science Institute, Tokyo Institute of Technology

In the field of astrophysics and planetary science, Computational Fluid Dynamics is an essential tool. Problems in these fields often contain inhomogeneities and various effects other than hydrodynamical pressure force, such as self-gravity. Since the Lagrangian method is suitable for dealing with these situations, to date, the Smoothed Particle Hydrodynamics (SPH) has been widely applied.

Recently, however, several critical issues of the standard SPH (SSPH) formulation have been reported. It is pointed out that SSPH has difficulties in dealing with hydrodynamical instabilities. To overcome this problem, several modifications to SSPH have been suggested and tested. As a result, previous works concluded that this issue is resolved. There is, however, another issue that SSPH cannot treat thin gas disk correctly. Since the disk structure is ubiquitous in the field of astrophysics and planetary science, this shortcoming is critical.

Recently, a novel particle-based numerical hydrodynamical simulation method, Weighted Particle Hydrodynamics (WPH), has been proposed. Through several numerical tests, it is demonstrated that WPH overcomes the known shortcomings in SSPH. WPH is an attractive particle-based hydrodynamical scheme.

WPH is, however, based on the Riemann Solver for the evaluation of the inter-particle fluxes. It is not easy to extend Riemann Solver to non-ideal equation of state, though methods exist. In some situations in the field of astrophysics and planetary science, we need to apply non-ideal equation of state. It is difficult to apply WPH to such a situation. In this work, thus, we use the artificial viscosity to WPH, instead of Riemann Solver. With the artificial viscosity we can use WPH for any functional form of the equation of state. In this work, we compare our new approach and the original WPH for hydrodynamical tests. We found that our new approach does not lose any advantage of WPH with Riemann Solver.

Keywords: methods: hydrodynamical, methods: numerical, protoplanetary disks

Chemical evolution of lunar magma ocean: evaluation of density overturn

HORI, Ayako¹ ; NAGAHARA, Hiroko^{1*}

¹Dept. Earth Planet. Sci., The Univ. Tokyo

Hess and Parmentier (1995) discussed gravitational instability of a highly fractionated heavy layer and proposed a mantle overturn model, which well explains the role as a source for high-TiO₂ mare basalts erupted several hundred millions years later. However, Hess and Parmentier (1995) themselves pointed out that the timescales for the IBC layer formation is longer than the onset of gravitationally instability between the IBC layer and underlying mantle, so the density instability should have resolved during LMO differentiation with small scale overturn. We constructed a model that describes differentiation of interstitial melt trapped in the cumulate layer with three parameters, critical crystal fraction, porosity of the cumulate layer, and grain size, and the percolation is evaluated as the time to the onset of instability between lighter trapped melt and the overlying heavier residual melt in the magma ocean body.

The results show that the density contrast between LMO and the trapped melt becomes significantly large once plagioclase appears, on the other hand viscosity of the melt is. The percolation time varies by up to about two orders of magnitude for the variation of porosity by two times, whereas it varies by up to about 5 orders of magnitude for the variation of grain size by one orders of magnitude, and the effect of X is not essentially. Comparing the percolation time at the critical crystal fraction for each step of differentiation calculation and the duration of the whole LMO crystallization, we can conclude that the percolation time is much shorter than the crystallization time if the grain size is larger than 1.0 cm. If we assume that the grain size of crystallizing grains in LMO is 0.1 to 1 cm in order, which is the average size in terrestrial magmas, melt overturn between LMO and trapped melt takes place easily during crystallization of LMO, which would make formation of extremely dense layer below the anorthosite crust at the final stage of LMO crystallization difficult.

Keywords: The Moon, magma ocean, density overturn Hess and Parmentier (1995) discussed gravita

Partitioning of sulfur between core and mantle on early Mercury and its building materials

SASAMORI, Eri^{1*} ; KURAMOTO, Kiyoshi¹

¹Hokkaido University, Graduate school of Science

Owing to its large density, the planet Mercury is believed to have a large metallic core covered with a relatively thin rocky mantle. Recently, measurements by MESSENGER's X-ray and gamma-ray spectrometers have revealed the Mercury's surface composition (Nittler et al., 2011, Evans et al., 2012). One of its most unexpected findings is the high sulfur abundance as much as 1.9-2.7 wt% because sulfur is in general depleted in the lithosphere of a rocky planet due to the preferential partitioning to molten metal that segregated to form a planetary core. Therefore, it is an open question why Mercury has such a large amount of sulfur in its surface material. On the other hand, the measured surface iron abundance is 1.6-2.2 wt%. If all iron forms oxide, this abundance is equivalent to 2.1-2.8 wt% of FeO, which is much smaller than those in the crusts of Earth and Mars and consistent with ground-based observations of Mercury's reflectance spectra. From the comparison of the oxidation state of iron, Mercury has been speculated to be formed from FeO-depleted building materials like enstatite chondrite (EC) (Wasson, 1988).

If Earth's geochemistry is simply applied for Mercury, the sulfur abundance in the lithosphere is expected to be very low. However, it has been known that sulfur becomes more soluble into silicate melt under reduced conditions depleted in FeO. Therefore, the extremely high abundance of sulfur on the surface of Mercury might come from sulfur partitioned to silicate melt when the Mercury's core formed.

Here, we study partitioning of sulfur between core and mantle during the formation of Mercury by using an empirical sulfide capacity model (Taniguchi et al. 2010) and attempt to estimate the Mercury's building materials from its surface composition. For the description of sulfur partitioning, the oxygen fugacity fO_2 and sulfur fugacity fS_2 are important. They are calculated by considering chemical equilibrium between silicate melt and metallic melt. The starting composition of Mercury's building material is prepared from the mean composition of EC. The silicate melt is the mixture of oxides and non-Fe sulfide components and the metallic melt is the mixture of metallic iron and iron sulfide components with keeping relative elemental abundances in EC, respectively. This will be referred to as the standard composition. In order to analyze compositional dependence, the ratios of FeO/S, [non-Fe sulfide]/Si in starting silicate melt and S content in starting metallic melt are varied, respectively. The pressure dependence is also estimated over 1-10 GPa from the volume changes of the partitioning reaction. The temperature is assumed to be 2000 K.

Given the standard composition, the equilibrium sulfur and FeO concentrations in silicate melt are estimated to be 1.6 wt% and 0.024 wt%, respectively. Compared with the Mercury's surface composition, the calculated sulfur content is fairly consistent whereas the FeO content is too small to account for the observed iron content. The sulfur content in silicate melt decreases when FeO/Si ratio increases and FeO content decreases when [non-Fe sulfide]/Si ratio increases. Furthermore, FeO content increases up to about 0.06 wt% when the sulfur content in metallic melt increases to about 50 mol% while the sulfur content in silicate melt little changes. The sulfur content in silicate melt is almost independent of pressure but the FeO content decreases as the pressure increases.

The sulfur content observed in Mercury's surface can be explained by wide range of building material compositions near EC. This supports the idea that Mercury was made from EC-like materials whereas the corresponding FeO content is too small to account for the observed iron content. Iron might have been additionally accreted on the surface of Mercury after core formation. Alternatively, a large impact might excavate metallic iron beneath the thin mantle and disperse its fragments over the Mercury's surface.

Keywords: Mercury, sulfur, partitioning

Metal-silicate partitioning of chlorine: Implications for the origin of terrestrial missing chlorine

KUWAHARA, Hideharu^{1*} ; GOTOU, Hirotada² ; OGAWA, Nobuhiro³ ; YAMAGUCHI, Asuka³ ; ISHIBASHI, Ko⁴ ; YAGI, Takehiko⁵ ; SUGITA, Seiji⁵

¹Graduate School of Frontier Sciences, The University of Tokyo, ²Institute for Solid State Physics, The University of Tokyo, ³Atmosphere and Ocean Research Institute, The University of Tokyo, ⁴Planetary Exploration Research Center, Chiba Institute of Technology, ⁵Graduate School of Science, The University of Tokyo

The chlorine abundance of the bulk silicate Earth may be depleted relative to the predicted values from various types of primitive materials, such as chondrites (Sharp & Draper, 2013). Such terrestrial missing chlorine would have been caused by planetary accretion processes. There are two hypotheses for the depletion of terrestrial chlorine; Incorporation into the Earth's core and primordial ocean blow off. The latter case is due to the high hydrophilic nature of chlorine. Here we experimentally examine the possibility of the former case. More specifically, metal-silicate partitioning of chlorine in a magma ocean is investigated.

Metal-silicate partitioning behavior of elements is controlled mainly by temperature, pressure, and oxygen fugacity of magma oceans. In this study, we first investigated the oxygen fugacity dependency for the partitioning coefficient of chlorine. Starting materials were prepared from a mixture of high-purity oxides (SiO₂, Al₂O₃, CaO, MgO) and metal (Fe). The relative abundances of each component in the mixture were assumed to be CI chondrite. Chlorine was added to the mixture as FeCl₂ (2wt.%). Oxygen fugacity was controlled by adding metallic Si to the samples. The starting materials were enclosed in graphite capsules. The experiments were performed at 4GPa and 1900K for 15 min using multi-anvil high pressure apparatus at Institute for Solid State Physics, The University of Tokyo. The sample was quenched by turning off the power to the heater. The elemental composition of recovered samples were analyzed by wavelength-dispersive electron microprobe at Atmosphere and Ocean Research Institute, The University of Tokyo.

The metal-silicate partitioning coefficient of chlorine in recovered samples was within the range between 0.001~0.01, suggesting that chlorine is a highly lithophile element. In addition, oxygen fugacity dependence on the partitioning coefficient was not observed. If such a highly lithophilic behavior of chlorine observed in our study does not depend significantly on pressure, terrestrial missing chlorine might require primordial ocean blow off during the main-accretion phase.

Reference: Sahrp, Z.D. and D.S. Draper, 2013, Earth Planet. Sci. Lett. 369-370, 71-77.

Keywords: Chlorine, Partitioning of elements, Primordial oceans, Core composition

Experimental study on propagation process of impact-induced seismic wave in quartz sand

MATSUE, Kazuma^{1*}; ARAKAWA, Masahiko¹; YASUI, Minami¹; MATSUMOTO, Eri¹; TSUJIDO, Sayaka¹; TAKANO, Shota¹; HASEGAWA, Sunao²

¹Graduate School of Science, Kobe University, Japan, ²Japan Aerospace Exploration Agency, JAXA

Introduction:

Recent spacecraft surveys clarify that the asteroid surface is covered with regolith made of boulders and pebbles such as that found on asteroid Itokawa by the Hayabusa spacecraft. The surface morphologies of asteroids formed on a regolith layer were found to be modified. For example, high-resolution images of asteroid Eros surface revealed the evidence of downslope movement of a regolith layer, then it could cause the degradation and the erasure of small impact crater. One possible process to explain these observation is the regolith layer collapse caused by seismic reverberation after projectile impacts (Richardson et al.2004, 2005). The impact-induced seismic activity might be the important physical process which affected the morphology change of asteroid regolith surface. Therefore, it is important for us to know the relationship between the impact energy of the projectile body and the impact-induced seismic energy. McGarr et al(1969) conducted the high-speed impact experiments on the loose sand target simulating the lunar surface in order to confirm the detectability of asteroid impacts on the lunar surface by seismographs set on the moon by the Apollo mission. Yasui et al. (in prep) conducted impact experiments at 100m/s on the glass beads target with the mean diameter of 200 μ m by using various projectiles and studied the decay process of impact-induced seismic wave to clarified the energy transfer efficiency from the impacting projectile to the seismic wave. It is important to study the dependence of the energy transfer efficiency on the different target materials and the impact velocity. So in this study, we carried out impact cratering experiments to observe the seismic wave propagating through the target far from the impact crater in different conditions that the quartz sand target was used and the impact velocity was extended up to 7km/s.

Experimental method

Impact cratering experiments were conducted by using a single stage vertical gun set at Kobe University and a two-stage vertical gun set at Japan Aerospace Exploration Agency (JAXA). The impact velocity was 200m/s for a single-stage gas gun, 1.5-6.9km/s in a two-stage gas gun. We used a quartz sand with the particle diameter of 500 μ m, density of 1.48g/cm³. The spherical polycarbonate projectile with the diameter of 4.75mm and the density of 1.2g/cm³ was used. The target was set in a large vacuum chamber below 10 Pa. The three accelerometers with the charge sensibility of 5.47pC/ms⁻² and the frequency response of 0.5Hz-10kHz was set on the target surface at different distances from the impact point. The acquired acceleration data of the acceleration were recorded by a data logger with A/D conversion rate of 100 kHz.

Result:

The waveform of impact-induced acceleration recorded by the accelerometers has a single peak and attenuates with time. It is noticeable that the peak value of the acceleration varies with the propagation distance, and the impact-induced seismic wave is found to attenuate with the propagation distance. The maximum acceleration, g_{max} , has a good relationship to the normalized distance x/R , where x is propagation distance and R is crater radius: $g_{max} = 160(x/R)^{2.98}$, irrespective of the impact velocities for the quartz sand. Furthermore, we examined the propagation velocity of the seismic wave by using the traveling time from the impact point. The seismic wave velocity was obtained to be 75 ± 15 m/s for the quartz sand.

Application to asteroid:

According to Richardson et al.2004, the critical physical condition to cause the surface morphology changes can be described by the acceleration of the regolith particles exerted by the seismic wave, and the condition is that the acceleration is greater than the surface gravity acceleration. By determining the distance x where g_{max} is the same as the surface gravity, it is possible to estimate the region where the surface morphology could change when the projectile body is impacted.

Keywords: impact, cratering, impact-induced seismic wave, regolith layer

Thermal conductivity model for powdered materials under vacuum

SAKATANI, Naoya^{1*} ; OGAWA, Kazunori²

¹ISAS/JAXA, ²Kobe University

Powdered materials have been ubiquitously existed in the solar system from the past to the present. For example, in early solar nebula, km-sized bodies so-called planetesimals are considered to have formed by accretion of dust particles. At present, surface of the Moon and asteroids are covered with crushed rock powders, called regolith. It is known that the powdered materials have lower thermal conductivity than intact materials by more than two orders of magnitude under vacuum condition. Therefore, even if the regolith covers a planetary body with thin thickness, it strongly affects the thermal evolution. The thermal conductivity of powdered materials under vacuum depends on several parameters (temperature, particle size, porosity, compressional stress, etc.), and varies by an order of magnitude, depending on the parameters. Since powdered materials on planetary bodies have various physical parameters, construction of an integrative thermal conductivity model describing these parameter dependences is of importance to address thermal problem of the planetary bodies.

Until now, we have experimentally investigated the parameter dependences of the thermal conductivity of powdered materials under vacuum, mainly using glass beads as analogous samples. Heat transfer mechanism in the powdered media has been studied based on the experimental results. In this presentation, we introduce a theoretical model of the thermal conductivity.

Previous studies for the thermal conductivity of powdered materials suggested several models. Some researchers modeled sphere beds with regular packing structures such as simple cubic packing, others suggested empirical models determined from experimental data. However, these models were not completely based on the physical mechanism. Moreover, they were incapable of reproducing the experimental results accumulated from previous experimental studies, and thermal conductivity values estimated from the models sometimes differed by one order of magnitude. Thus, it had been hard to estimate the thermal conductivity of powdered materials on planetary bodies accurately.

We first constructed the first quantitative model of the thermal conductivity of powdered materials in accordance with physical and heat transfer mechanisms successfully, by assuming random packing of mono-sized spheres. Our model integratively describes the parameter dependences, such as temperature, particle size, porosity, compressional stress, etc. By giving values of these parameters, we can estimate the thermal conductivity of powdered materials with various physical conditions. By comparing the model with experimental data for glass beads we obtained, it was found that our model could predict maximum values, and that the relative differences were less than factor of three.

Keywords: thermal conductivity, powdered material

An iterative method for determining temperature distribution of a spherically symmetric body in a planetary system

SEKIYA, Minoru^{1*} ; SHIMODA, Akihito²

¹Department of Earth and Planetary Sciences, Faculty of Sciences, Kyushu University, ²Department of Earth and Planetary Sciences, Graduate School of Sciences, Kyushu University

A semi-analytical iterative method for determining the temperature distribution in a spherically-symmetric body with spin motion and eccentric orbital motion is developed. The formulas for determining the change rates of orbital elements due to the Yarkovsky effect are also developed. The advantage of this work compared to Sekiya and Shimoda (2013) is that the effect of the eccentric orbit is taken into account. The advantage of this work compared to Vokrouhlicky and Farinella (1999) is that the temperature dependence on the longitude is taken into account without assuming the symmetry with respect to the rotation axis. We can calculate the temperature distribution as a function of the colatitude, the longitude, and the mean anomaly with arbitrary precision by continuing the iterative method, as long as the eccentricity is less than about 0.7. The details are written in Sekiya and Shimoda (2014).

References:

- Sekiya, M. and Shimoda, A.A. (2013) *Planetary and Space Science*, 84, 112-121.
- Sekiya, M. and Shimoda, A.A. (2014) *Planetary and Space Science*, 97, 23-33.
- Vokrouhlicky, D. and Farinella, P. (1999) *Astronomical Journal*, 118, 3049-3060.

Keywords: asteroid, solar system, planet, meteorite, celestial mechanics, orbit

Impact velocity dependence of transient crater growth in granular targets

YAMAMOTO, Satoru^{1*} ; HASEGAWA, Sunao² ; SUZUKI, Ayako² ; MATSUNAGA, Tsuneo¹

¹NIES, ²JAXA

In this study, we developed a new method for direct observations of transient crater growth in granular targets using a laser profiler. This method allows us to measure the excavation cavity in the transient crater growth at a temporal resolution of ~1 ms without using a high-speed video camera. Using a vertical two-stage light gas gun at JAXA, we conducted impact cratering experiments onto granular targets. Using the laser profiler, we successfully obtained the time expansion data of the excavation cavity for the impact velocities ranging from ~0.8 km/s to 6 km/s. Based on these new data for the transient crater growths, we discuss how the scaling law for impact cratering in the gravity regime depends on impact velocity.

Keywords: impact crater, impact experiment, scaling law, gravity regime

Morphologies of impact craters formed on spherical gypsum

SUZUKI, Ayako^{1*} ; KUROSAWA, Kosuke² ; HASEGAWA, Sunao¹ ; HIRAI, Takayuki¹ ; OKAMOTO, Chisato³

¹ISAS/JAXA, ²PERC/Chitech, ³Graduate School of Science, Kobe University

1, Introduction

Impact cratering processes on small bodies are expected to be different from those on large planets because small bodies possess unique properties which affect impact cratering processes, such as high porosity (e.g., Britt et al., 2002), low gravity, small impact velocity (e.g., Bottke et al., 1994; Marchi et al., 2013), and irregular surface against crater size (Sullivan et al., 2002).

Many craters on irregular surfaces are observed on asteroids, such as Ida, Eros, and Itokawa, through the recent planetary exploration missions.

Fujiwara et al. (1993, 2014) produced distinctive-shaped impact craters on spheres and cylinders with a wide range of its radius in a laboratory, and presented the empirical relations between crater diameters/depths and the target curvature. In this study, we present the results of a series of impact experiments using spherical targets. The crater profiles on the spherical surfaces were measured with a higher accuracy than those obtained in the previous studies. Then, we propose a physical mechanism how the target curvature affects the crater volumes.

2, Experiments

Impact experiments were performed by using a two-stage light-gas gun at the facility of ISAS/JAXA. The two types of gypsum targets were used. One is a cube with ~9 cm on a side, and the others are spheres with 7.8 cm, 10.9 cm, 17.0 cm, and 24.8 cm in diameter. The bulk density and tensile strength of the target was 1.05 g/cm³ and 2.03 MPa, respectively. A projectile was a nylon sphere with 3.2 mm in diameter, and impacted into the target at ~3.3 km/s. The targets were placed in a box made of styrofoam, and the box was placed in a vacuum chamber. After each shot, the target and their fragments were collected from the box. Then, the spherical surface including a resultant crater was scanned by a high resolution 3-D geometry measurements system (COMS MAP-3D). The volume of the crater was measured with the deviation from the spherical surface which determined by using the topographic data around the crater.

In addition, we used the iSALE shock physics code (Amsden et al., 1980; Ivanov et al., 1997; Wunnemann et al., 2006), to investigate the effects of target curvature on the pressure distribution in the target..

3, Results and discussion

The resultant craters consist of a centered pit and a spall zone which encompasses the pit. A larger target curvature led to a broader the spall zone. The volume and the diameter of the crater increase as the target curvature increases, although the depth of the crater is almost constant. The volume of the crater formed on the 7.8-cm spherical gypsum, which has the largest curvature, is 3.5 times larger than those formed on the cubed gypsum, while the pit volume of the crater on the 7.8-cm spherical gypsum is 1.8 times larger than those on the cubed gypsum. Crater profiles also show the spall zone becomes broader and deeper as the target curvature increases. The volume increase in the spall zone mainly contributes to the volume increase of the crater.

The distribution of the peak shock pressure in the targets is calculated by using the iSALE in a two-dimensional cylindrical coordinate. The attenuation behavior of an impact-generated shockwave should be controlled by the interaction between the shockwave and a rarefaction wave from the spherical surface. Since the geometry of free surface changes with the target curvature, the pressure distribution is likely to depend on the target curvature. Base on the results of such 2-D calculations, we found that a larger target curvature leads to a wider spallation zone produced by a pressure gradient from the deep interior to the spherical surface. This trend is qualitatively consistent with the experimental results.

Acknowledgements

We appreciate the developers of iSALE, including G. Collins, K. Wunnemann, B. Ivanov, J. Melosh, and D. Elbeshausen. We are grateful Dr. K. Goto and H. Toshima in ISAS/JAXA for supporting us to measure the tensile strength of gypsum.

Keywords: impact craters, impact experiments, gypsum, curved surface, morphology, two-stage light-gas gun

In-situ observations of the ablation processes of artificial shooting stars

KUROSAWA, Kosuke^{1*} ; SENSU, Hiroki¹ ; SUZUKI, Kojiro² ; KASUGA, Toshihiro³ ; SUGITA, Seiji⁴ ;
MATSUI, Takafumi¹

¹PERC/Chitech, ²Graduate School of Frontier Science, The Univ. of Tokyo, ³NAOJ, ⁴Graduate School of Science, The Univ. of Tokyo

We studied the aerodynamic ablation processes of small bodies entered into planets and/or satellites with a thick atmosphere. The kinetic energy of a small body is parted into the thermal energy and the kinetic energy of a shockwave propagated into a surrounding air during an atmospheric passage. Active chemical reactions between a vaporized impactor and the surrounding air are driven by the kinetic energy of the impactor. Since the extraterrestrial material mixes with the atmosphere, the induced chemical reactions have never been driven in the mean-field on the planets/satellites. Such events are expected to frequently occur through the history of the Solar system and may affect the atmospheric evolution on the planets/satellites. The energy partitioning and chemical reactions as mentioned above, however, has not been investigated well because it occurs via a number of complicated physical and chemical processes.

We have made artificial shooting stars using a two-stage light gas gun at a new laboratory of Planetary exploration Research Center of Chiba Institute of Technology (PERC/Chitech). A flight tube for accelerated projectiles and a chamber were filled with N₂ gas. Then, a plastic sphere was shot into the N₂ gas. A high-speed imaging observation and a time-resolved spectroscopic observation of an artificial shooting star, observed from two directions perpendicular to the projectile trajectory, were conducted simultaneously. The distance between the projectile trajectory and the collecting optics of measuring instruments was ~50 cm. We successfully resolved the spatial distribution of an artificial shooting star with the time and spatial resolution of 0.5 us and 100 um, respectively. The spatial structure of the shooting star, the distribution of produced gases, and the blackbody temperature along the trajectory were obtained. We are planning to investigate the elemental steps of the energy partitioning with the comparison between the experimental results and the prediction by a computational fluid dynamics.

Keywords: Small bodies, Shooting stars, Aerodynamic ablation, Two-stage light gas gun, High-speed imaging, Time-resolved emission spectroscopy

Orbit Determination of Meteoroids by MU Radar Meteor Head Echo Observations

ABE, Shinsuke^{1*} ; KERO, Johan² ; NAKAMURA, Takuji³ ; FUJIWARA, Yasunori⁴ ; WATANABE, Jun-ichi⁵ ;
HASHIGUCHI, Hiroyuki⁶

¹Department of Aerospace Engineering, Nihon University, ²Swedish Institute of Space Physics (IRF), ³National Institute of Polar Research, ⁴The Graduate University for Advanced Studies, ⁵National Astronomical Observatory, ⁶Research Institute for Sustainable Humanosphere, Kyoto University

The various mass ranges of meteoroids ranging between 10-15 and 1015g are continuously colliding with the Earth. Most of them are so called micrometeoroids, micrometeorites or IDPs (Interplanetary Dust Particles) whose diameters are estimated between 10 and several 100 micrometres. It is indicated by radar, high-flying aircraft and zodiacal cloud observations that a daily mass influx of meteoroids is ranging from 100 to 300 tones. However, it is still a matter of finding parent bodies of most meteoroids, while parent bodies for the most of major meteor showers have been identified as comets or dormant comets. Their physical and chemical aspects such as composition, structure as well as their origins are also poorly known. The influx rate of interplanetary dusts and artificial space debris onto the Earth's surface are essential for the human space activities. Thus, it is very important to investigate influx, orbits and mechanical strength of meteoroids that can be observed as meteors after interacting with the upper atmosphere.

High power large aperture (HPLA) radar observation is a recent technique to provide useful information on meteor influx and orbits, as well as interactions with the atmosphere. The recent development of the technique carried out using the middle and upper atmosphere radar (MU radar) of Kyoto University at Shigaraki (34.9N, 136.1S), which is large atmospheric VHF radar with 46.5 MHz frequency, 1 MW output transmission power and 8330 m² aperture array antenna, has established very precise orbital determination from meteor head echoes. More than 150,000 meteor orbits have been measured since 2009.

In this study, we present the physical quantities of meteoroids such as orbital parameters, flux rate and ablation characteristics obtained from the MU radar meteor head echo observations. The origin and internal structure of meteoroids compared with comets, asteroids and space debris will be discussed.

Keywords: Meteors, Asteroids, Comets, Radar

Planetesimal size and turbulence strength in a protoplanetary disk

KOBAYASHI, Hiroshi^{1*} ; TANAKA, Hidekazu² ; OKUZUMI, Satoshi³

¹Nagoya University, ²Institute of Low Temperature Science, Hokkaido University, ³Graduate School of Science, Tokyo Institute of Technology

We investigate the collisional evolution of bodies with radius from 1 to 1000 km in a turbulent disk. The growth of small bodies is affected by turbulence. Once bodies get larger and turbulence is negligible, large bodies start runaway growth. Therefore, the size distribution depends on the strength of turbulence. The size distribution is directly related to that of minor bodies in the Solar System and affects subsequent planet formation.

Keywords: planet formation, planetesimal, asteroids, comets

Structure of the accretion disk around a protostar and the planetesimal formation (I)

EBISUZAKI, Toshikazu^{1*} ; IMAEDA, Yusuke¹

¹RIKEN

”Headean Bioscience” has started the budget year 2014 by Kekenhi: Scientific Research on Priority Areas. A05 Life planet group aims to study the formation process of life planets like the Earth.

We constructed a steady state 1-D model of a protoplanetary disk taking into account of the magneto-rotational instability (MRI) and photo-evaporation by the ionizing radiation from the central stars. We found that a quiescent zone appears in 0.5AU-5AU and sandwiched by inner and outer turbulent regions. The column density of the quiescent zone is one order of magnitude higher than the other part of the disk. Two boundaries of quiescent zone is promising sites of the planetesimal formation site accumulating the solid particles.

When accretion rate decrease down to 10^{-8} solar mass per year, the near side of the disk gas will dissipate by the photo-evaporation. We will present the research strategy of the A05 Life planet group and major results.

Keywords: protoplanetary disk, planetesimal formation, magnetorotational instability

The thermal structure of the hybrid-type proto-atmosphere of Mars growing in the solar nebula

SAITO, Hiroaki^{1*} ; KURAMOTO, Kiyoshi¹

¹Cosmo Sci., Hokkaido Univ

According to meteorite chronology, Mars has reached the half of its present mass as within 3 Myr (Dauphas et al., 2011). Since this time scale is much shorter than the estimated lifetime of the solar nebula, the accretion of Mars mostly proceeded within the solar nebula. On the other hand, the energy released by planetesimal collision becomes large enough to induce degassing of the volatile compounds such as H₂O when the proto-Mars gets larger than lunar size (0.1 M_{Mars}). Therefore, growing Mars may have had a proto-atmosphere consist of nebula gas and degassed gas, which is referred as to hybrid-type proto-atmosphere.

In this study, we analyze the thermal structure of hybrid-type proto-atmosphere by building a 1D radiative-convective equilibrium model. Here we assume an atmosphere that consists of two layers: the upper one is dominated by the solar nebula components and the lower one is dominated by degassed components. These layers are unmixed because of their density gap and their boundary is referred as to compositional boundary. The higher the compositional boundary altitude, the larger the mass of degassed components. The degassed components are comprised of H₂, H₂O, CH₄ and CO. The mixing ratio of these molecular species is taken from Kuramoto (1997) that calculates thermochemical equilibrium among fluid, silicate melt and molten metallic iron. Radiative transfer is modeled by taking into account the absorptions by H₂, He, CH₄, CO and H₂O. The effect of H₂O condensation is incorporated for vertical compositional profile and the adiabatic lapse rate. The pressure and temperature of the solar nebula on Mars orbit are adopted from Kusaka et al. (1970). Radiative-Convective equilibrium structures are obtained as a function of accretional heating rate and the amount of degassed component. The accretion time is taken 1 - 6 Myr compatible with the chronology of Martian meteorites and the accretion rate is assumed to be constant.

We first study the dependence of the temperature structure on the mass of degassed component by changing the altitude of compositional boundary. For the pure nebula atmosphere, the surface temperature does not exceed 700 K (Hayashi et al., 1979). As the mass of degassed component increases, the surface temperature also increases. This is because both the mean molecular weight and mean absorption coefficient of degassed component are larger than of the solar nebula components. In our model setting, the surface temperature of Mars exceeds the melting point (1500K) at the final growth stage if the mass of degassed component is more than 1% of the Mars mass and the accretion time is within 6 Myr,

In addition, we analyzed the surface temperature of Mars at each growth stage (0.1 M_{Mars} - 1 M_{Mars}) by fixing the mass ratio of degassed atmosphere to the bulk of growing Mars. When the mass ratio is larger than about 1% or less than 0.001%, the surface temperature increases with the mass of proto-Mars. On the other hand, the mass ratio is between about 0.001 - 1 %, the surface temperature can sometimes decrease with increasing Mars mass. This behavior is likely related to switching the relative locations of compositional boundary and tropopause.

Gravitational instability by suppression of magnetic turbulence by electric-field heating

MORI, Shoji^{1*}; OKUZUMI, Satoshi¹

¹Graduate School of Science, Tokyo Institute of Technology

Turbulence in protoplanetary disks is essential for disk evolution since the turbulence transport angular momentum outside and the gas falls into the central star. One of possible mechanism of generating the turbulence is magnetorotational instability (MRI; Balbus & Hawley 1991). In a region far from the star where MRI fully develops, electric fields induced by MRI will heat up electrons (electric-field heating; Inutsuka & Sano, 2005). When the electric-field heating occurs, heated electrons tends to collide with and be captured by dust grains. Since number density of electrons decreases in the gas-phase, finally magnetic fields may disperse (Okuzumi & Inutsuka, 2015). For MRI, the dispersion of magnetic fields implies suppression of the magnetic turbulence. We have investigated where and how MRI turbulence is suppressed in protoplanetary disks so far. As a result, we have estimated the MRI turbulence is suppressed within approximately 100 AU on the mid-plane (electric-field heating region; the fall meeting of the Japanese Society for Planetary Sciences, 2014).

The purpose in this study is to investigate where the gas is accumulated in the disk considering electric-field heating.

In a vigorous turbulent region, the turbulence transports angular momentum of gas and the gas falls into the central star. On the other hand, in a weak turbulent region, accretion gas from outer disk is accumulated because of inefficiency of angular momentum transport. Therefore, the broad suppression of MRI turbulence will change the global disk structure of surface density (Mori & Okuzumi, in prep.). The fallen gas is accumulated in the inner region where MRI does not grow (dead zone; Gammie 1996), and the possibility is pointed out that gravitational instability occurs in the region. Considering the electric field heating of our study, the gas will be accumulated in broader region.

We calculated the relation between surface density and mass accretion rate at each place in disks. As our disk model, we set the disk containing 0.1 μm -sized dust grain with dust-to-gas mass ratio of 0.01, and the gas pressure to the magnetic pressure on the mid-plane to be 10^4 . As a result, with the mass accretion rate of $10^{-7} M_{\odot}/\text{yr}$, *the surface density realizing the steady accretion does not*

Keywords : protoplanetary disk, MHD, magnetorotational instability, gravitational instability, accretion disk

Impact of eccentricity damping on the migration of a giant planet

UEDA, Takahiro^{1*} ; IDA, Shigeru² ; TAKEUCHI, Taku¹

¹Department of Earth and Planetary Sciences, Tokyo Institute of Technology, ²Earth-Life Science Institute, Tokyo Institute of Technology

Recently, the gravitational instability (GI) model has been revisited as the formation of giant planet and brown dwarf because of the detection of long-period giant planets with small eccentricity (e.g. Marois et al. 2010). With GI, giant planet is formed by the fragment of a gravitationally unstable disk which has a few to tens of Jupiter mass and large semi-major axis above 50AU. We have investigated the migration of a giant planet initially in wide orbit considering eccentricity damping and gravitational turbulence directly integrating the equation of motion numerically. Firstly, we have examined the effect of eccentricity damping. When there is a relative velocity between planet and surrounding disk gas, which means planet has the eccentric orbit, gravitational interaction which is known as “Dynamical Friction” arises between them. As a consequence, eccentricity damps to $e = 0$. We found that for planet with wide orbit, during eccentricity damping, we can assume the conservation of angular momentum, even if the torque is always exerted on the planet. In other words, semi-major axis and eccentricity almost decrease due to energy dissipation. If planets have large eccentricity, planet can migrate faster than Type I migration due to eccentricity damping. In addition, we have investigated the effect of gravitational turbulence. For the random forces due to disk turbulence, we used the semi-analytical formula developed by Laughlin et al.(2004) and modified by Ogiwara et al.(2007) with slight modification. As a result, we found that gravitational turbulence cannot excite planet’s eccentricity to $e \gg H/r$. Therefore, it can be said that gravitational turbulence is not important to the migration of a giant planet.

Keywords: giant planet, migration, disk-planet interaction

Effect of wave propagation for a planet-induced gap formation in protoplanetary disks

KANAGAWA, Kazuhiro^{1*} ; MUTO, Takayuki² ; TANAKA, Hidekazu¹ ; TANIGAWA, Takayuki³ ; TAKEUCHI, Taku⁴

¹ILTS, Hokkaido University, ²Division of Liberal Arts, Kogakuin University, ³School of Medicine, University of Occupational and Environmental Health, ⁴Department of Earth and Planetary Sciences, Tokyo Institute of Technology

In a protoplanetary disc, a large planet is able to create the so-called disc gap, which is a low gas density region along with the planetary orbit, due to the gravitational interaction between the disc and the planet. The gap formation significantly affects the orbital evolution of planets such as the transition from type I migration to type II migration. It also prevents disc gas from accreting onto the planet and slows down the planetary growth. In addition, the gap formation induced by a giant planet possibly explains the formation of the so-called pre-transition disc with a ring gap. Hence, it is important to determine the relation between the planet mass and the gap depth and width.

According to our analysis with the one-dimensional model, the propagation and damping of the density wave excited by the planet is closely related to the gap depths and widths (Kanagawa et al 2015). Therefore, we computed the gap structure around the planet using FARGO, which is an open source code for hydrodynamic simulation. Results of the simulation show that in the case with the large planet (such as Jupiter), low-mode waves (in particular $m=2$ mode) become stronger than high-mode waves. Because the low-mode waves would be difficult to be damped by shock dispersion, these waves can propagate farther from the planet than high-mode waves.

In this talk, I will illustrate the results and discuss the wave propagation and gap formation for large planets.

Keywords: protoplanetary disk, disk-planet interaction, disk evolution

On Shortwave Emission from Accreting Gas-Giant Planets

AOYAMA, Yuhiko^{1*} ; TANIGAWA, Takayuki² ; IKOMA, Masahiro¹

¹Department of Earth and Planetary Science, Graduate School of Science, The University of Tokyo, ²School of Medicine, University of Occupational and Environmental Health

Planets have been thought to form in circumstellar gaseous disks (or protoplanetary disks), which are remnants of star formation. Some young stars surrounded by protoplanetary disks are already detected. Also, Atacama Large Millimeter/submillimeter Array (ALMA) has recently detected gap-like structure in a protoplanetary disk, which may be formed as a consequence of gravitational interaction between the disk and unseen planets. A challenging issue is how to find growing planets in protoplanetary disks directly. In this study, we investigate whether detectable emission occurs from accreting gas-giant planets.

In the core accretion models for formation of gas giant planets, a solid core with the critical core mass starts to get disk gas in a runaway manner. In this phase (called the runaway gas accretion phase), gas flows into the planet from the protoplanetary disk at a high accretion rate. Since the accretion of disk gas occurs much faster than loss of the angular momentum of the disk gas, a circumplanetary disk, which extends to the planet's Hill radius, is formed in the mid-plane of protoplanetary disks. Recent three-dimensional hydrodynamic simulations by Tanigawa et al. (2012) revealed that the disk gas flows into the circumplanetary disk not horizontally through the Lagrange points from the protoplanetary disk, but vertically from high altitudes. According to those simulations, the disk gas falls onto the circumplanetary disk with a speed comparable to the free fall speed, and the local gas temperature reaches up to tens of thousands of kelvin because of shock heating near the planet.

Thus, the presence of an accreting gas giant planet in a protoplanetary disk may be found by observing the radiative emission from such hot gas in the circumplanetary disk, which we aim to confirm in this study. Based on Tanigawa et al. (2012), we estimate the temperature of the gas heated by the accretion shock and simulate the thermal emission spectrum. In particular, we evaluate the detectability of the intensity of line emission from hydrogen. We have found, for example, that the Lyman-alpha luminosity from the circumplanetary disk is on the order of 1021 [W] in the case of an accreting gas-giant planet with mass of 130 Earth masses orbiting 5.2 AU in the minimum-mass solar nebula. The value of the Lyman-alpha luminosity is comparable to that from the present Sun. Since this luminosity is proportional to the density of disk gas, the emission continues until the dissipation of the disk gas. Considering the absorption by the interstellar medium and the protoplanetary disk gas, we discuss the detectability of forming gas giant planets for future space telescopes.

Keywords: Planet Formation, Gas-Giant Planet, Exoplanet, Direct Detection

Five Years of SEEDS: Direct Imaging of Exoplanets and Disks with Subaru

TAMURA, Motohide^{1*} ; SEEDS, Team¹

¹The University of Tokyo, Graduate School of Science

SEEDS (Strategic Explorations of Exoplanets and Disks with Subaru) is the first Subaru Strategic Program, whose aim is to conduct a direct imaging survey for giant planets as well as protoplanetary/debris disks at a few to a few tens of AU region around 500 nearby solar-type or more massive young stars devoting 120 Subaru nights for 5 years. The targets are composed of five categories spanning the ages of ~ 1 Myr to ~ 1 Gyr. Some RV-planet targets with older ages are also observed. The survey employs the new high-contrast instrument HiCIAO, a successor of the previous NIR coronagraph camera CIAO for the Subaru Telescope. We describe the outline of this survey and present its main results. The results includes discovery and characterization of 4 planets via direct imaging. detection of more than 2 brown dwarfs, discovery of companions around more than 2 RV-planetary systems. We also report the discovery of unprecedentedly detailed structures of about 20 protoplanetary disks and some debris disks. The detected structures such as wide gaps and spirals arms of a Solar-system scale could be signpost of planet.

Keywords: exoplanet, disk, direct inaging, infrared

Hydrodynamic escape from GJ 1214b atmosphere

WATANABE, Kensuke^{1*} ; KURAMOTO, Kiyoshi¹

¹Department of CosmoSciences, Graduate School of Sciences, Hokkaido University

The extra-solar planet GJ 1214b discovered in 2009 has a radius 2.7 times the Earth's radius and a mass 6.5 times the Earth's mass, and its mean density is 1.9 g/cm^3 which is a value intermediate between those of rock and ice. Therefore, the GJ 1214b was possibly born as a giant ice planet, and might have acquired a hydrogen envelope during its formation like Neptune. On the other hand, a recent transit observation (i.e. Kreidberg et al., 2014) suggests that GJ 1214b has an atmosphere which consists of gas with high mean molecular weight. This implies that almost all hydrogen has been lost from this planet due to hydrodynamic escape driven by stellar EUV (Extreme Ultra Violet) radiation.

Recently, Lammer et al. (2013) numerically investigated the hydrodynamic escape from GJ 1214b assuming a hydrogen-rich atmosphere under the present EUV flux from the parent star. They obtained an escape rate smaller than 10 % of the observational estimation for HD 209458b, a hot Jupiter surrounded by expanding hydrogen gas (Vidal-Madjar et al., 2003). This result implies that the mass of GJ 1214b little changes through the planet history and the hydrogen envelope, if once acquired, would be maintained at present. However, their numerical solution shows significantly small escape flux compared with the energy-limit escape rate and its reason was unexplained. Their study has heating profile suggesting that incident EUV radiation is almost completely absorbed by the atmosphere before it reaches the bottom of calculation region. However, the total energy absorbed by the entire atmosphere per unit time is an order of magnitude smaller than the total EUV energy supplied to the planet. Thus this study might have a problem with radiative transfer calculation and underestimate the escape rate.

In order to obtain more accurate estimation of escape rate and discuss the effect of hydrodynamic escape on GJ 1214b, we apply a numerical model of the time-dependent, inviscid hydrodynamic equations for a pure atomic hydrogen atmosphere in spherical symmetric geometry with CIP & CIP-CSL2 methods that have high accuracy for mass and energy conservation (modify Kuramoto et al., 2013). We confirm that our model almost exactly satisfies uniformity of mass flux and energy conservation. Given basically the same boundary conditions with Lammer et al. (2013) (the temperature and density at lower boundary are 475 K and $1 \times 10^{19} \text{ m}^{-3}$, respectively, and the incident EUV flux is 470 times the present solar), our model obtains hydrodynamic escape rates approximately 6-10 times larger than those by Lammer et al.'s study.

When we use the reevaluated hydrodynamic escape rate and the EUV flux dependent on the stellar age (Engle and Guinan 2011), the total mass of hydrogen escaped from GJ 1214b through the planet history is as large as approximately 15%-88% of the present planet mass. Therefore the hydrogen envelope of proto-GJ 1214b may have been almost completely lost, which is consistent with the observation suggesting hydrogen-depleted atmosphere. Furthermore, the initial mass of GJ 1214b is possibly as large as 1.15-1.9 times current mass (0.43-0.72 times the present Neptune mass), therefore this planet may have been more similar to Neptune in its mass and bulk composition in the past.

Keywords: Hydrodynamic escape, GJ 1214b

Climate modeling of an exoplanet possibly holding life GJ667Cc

NARITA, Kazuki^{1*} ; KURAMOTO, Kiyoshi²

¹Department of Earth Sciences, School of Science, Hokkaido University, ²Department of CosmoSciences, Graduate School of Sciences, Hokkaido University

In accord with the numerous discoveries of exoplanets in recent years, some studies on the habitability of exoplanets have been conducted by using global circulation models (GCMs) [e.g. Wordsworth et al., 2011; Leconte et al., 2013]. Among the exoplanets possibly holding liquid water on their surface like Earth, terrestrial planets that orbit around red dwarf stars are important as a target of such study because of their relatively high observational feasibility.

In consideration of these backgrounds, we carried out a climate simulation of the exoplanet GJ667Cc, whose ESI [earth similarity index] was the largest as of November 20, 2014, with dcpam5 [Takahashi et al., 2013], one of the GCMs. Considering its orbit and age, this planet orbiting a M-type star is likely to be under significant tidal locking action and accordingly rotates synchronously facing the same hemisphere to its central star. We also performed a simulation of Earth as a control experiment. Based on their results, we compare the simulated climate of GJ667Cc to that of Earth concerning the global average values of surface temperature and precipitation, their distribution related to the atmospheric circulation, and chemical weathering rate. We also estimate the timescale for H₂O localization on the night side. Then, possible climate state of GJ667Cc is speculated by combining these analyses.

Incident stellar radiation on the orbit of GJ667Cc is about 90% of the solar radiation on the Earth's orbit. Therefore the equilibrium temperature of this planet is about 7 K lower than that of Earth, if they have the same albedo. GJ667Cc has a radius 1.54 times the Earth's radius and a mass 3.8 times the Earth's mass. We conducted simulations assuming the surface gravity and the mass of atmosphere scaled from those of Earth in proportion to planetary mass and the atmospheric composition identical with that of the present Earth.

The average surface temperature of GJ667Cc experiment is about 40 K lower than that of Earth one and the average annual precipitation of the former one is about 320 mm less than that of the latter one, respectively. Distribution of precipitation, wind speed, and temperature shows that the day side of GJ667Cc is characterized by high temperature and intense precipitation around the substellar point, whereas the night side has cold poles at high latitudes surrounded by subtle precipitation. The circulation pattern is dominated by Hadley circulation reaching high latitudes on the day side with convection over the terminator, weak super rotation, and vortices around the cold poles on the night side. These characteristic structure of GJ667Cc experiment well explains the distribution of surface temperature and precipitation.

Chemical weathering rate of GJ667Cc experiment is estimated at about 5.8 times larger than that of Earth experiment, despite its lower average temperature and less precipitation. This was due to notably high temperature and intense rainfall at the substellar point and its surroundings. Chemical weathering is a process which consumes atmospheric CO₂. Given igneous CO₂ supply rate on GJ667Cc 3.8 times larger than that on Earth by mass scaling, consumption would exceed supply and thus the average surface temperature is expected to become lower than calculated value according to Walker feedback [Walker et al., 1981]. From the terminator to the entire night side, the surface temperature of GJ667Cc is continuously below the freezing point of H₂O. H₂O transported there could be fixed as ice, and therefore H₂O might be localized on the cold region. Given the total amount of H₂O on the surface of GJ667Cc by mass scaling, the timescale of H₂O localization is estimated to be about 18.7 million years based on the snowfall and frost flux in the cold region. Here we neglect the possible interaction between weathering and H₂O localization, which would prolong the localization timescale.

Keywords: exoplanets possibly holding life, GJ667Cc

A numerical experiment on dependence of the atmospheric structure of a synchronously rotating planet on planetary radius

ISHIWATARI, Masaki^{1*} ; MASUDA, Kazutaka¹

¹Hokkaido Univ. Graduate school of Science

In this study, a parameter experiment with a general circulation model (GCM) is performed in order to examine dependence of the climate of a synchronously rotating aquaplanet on planetary radius. Most of previous numerical studies on climates of exoplanets with mass similar to Earth's use experimental configuration imitating particular exoplanets, and parameter study with various values of planetary radius has not been performed. Heng and Vogt (2011) performs a numerical experiment with changing values of planetary radius and gravitational acceleration from 1.46 times of Earth's values to 1.71 times for the purpose of investigating the climate of Gliese581g. They show that surface temperature has its maximum value and minimum value at the subsolar point and anti solar point, respectively. However, the result may be changed with more large value of planetary radius, since the circulation pattern may change due to the decrease of radius of deformation compared to planetary radius. We examine the dependence of atmospheric structures for wide range of planetary radius.

The GCM utilized in this study is DCPAM5 (Dennou-Club Planetary Atmospheric Model; Takahashi et al., 2013). The governing equations for dynamical process are the primitive equations. For horizontal direction, the triangular truncation of the spectral transform method is used. As vertical axis, sigma is adopted. The surface of planet is entirely covered with ocean with zero heat capacity (swamp ocean). Earth's values are used for gravitational acceleration, dry air mass, and solar constant. For planetary rotation rate, an estimated value for Gliese 581g is adopted. For synchronously rotating planet configuration, the axial inclination is set to be zero, and the solar insolation distribution is fixed to the planetary surface. Values of planetary radius R^* (R^* is planetary radius normalize by Earth's value) is changed from 0.5 to 8.0.

The result of GCM experiment shows that surface temperature averaged over night side decreases with the increase of R^* . The value of the case with $R^*=1.0$ is 15 K lower than that of the case with $R^*=8.0$. In horizontal distribution of surface temperature, the value in high-latitudinal region of the night side decreases with the increase of R^* . On the other hand, surface temperature at the subsolar point increases with the increase of R^* . Subsolar surface temperature of the case with $R^*=1.0$ is 20 K higher than that of the case with $R^*=8.0$. The amount of day-night energy transport decreases with the increase of R^* , which is consistent with the increase of the difference of surface temperature between the day side and the night side. The results imply that a climate state with large spatial difference in surface temperature tends to appear in synchronously rotating planet with large planetary radius.

Keywords: exoplanets, synchronously rotating planets, planetary radius, general circulation model

Radius Anomaly of Hot Jupiters: Reevaluation of the Possibility and Impact of Layered-Convection

KUROKAWA, Hiroyuki^{1*} ; INUTSUKA, Shu-ichiro¹

¹Dept. of Phys., Nagoya University

Masses and radii are fundamental quantities to constrain the compositions of exoplanets. However, observations have revealed that a significant number of close-in gaseous planets (hot Jupiters) have anomalously large radii compared with the theoretical model of planets composed of hydrogen and helium (Baraffe et al., 2010; Baraffe et al., 2014). Understanding of the mechanism of the anomaly is crucial for the estimate of their compositions, and hence, crucial for constraining their formation histories.

Delayed contraction due to compositional inhomogeneity in their interiors has been proposed to explain the radius anomaly (Chabrier & Baraffe, 2007). The compositional inhomogeneity possibly inhibits large-scale-overturning convection and forms small-scale-layered convection which is separated by diffusive interfaces (Rosenblum et al., 2011; Mirouh et al., 2012; Wood et al., 2013). Inefficient heat transport of the layered convection creates a super-adiabatic temperature gradient, which results in the delayed contraction. Chabrier & Baraffe (2007) assumed the presence of the layered convection in the interiors of hot Jupiters, and demonstrated that its effect is sufficient to reproduce the radius anomaly.

However, the layer forms in a limited parameter range described by the reciprocal of the density ratio, $R\rho^{-1} = \alpha \mu \nabla \mu / \alpha_T (\nabla_T - \nabla_{ad})$, where $\alpha_T = -(\partial \ln \rho / \partial \ln T)_{p,\mu}$, $\alpha \mu = (\partial \ln \rho / \partial \ln \mu)_{p,T}$, $\nabla_{ad} = (\partial \ln T / \partial \ln p)_{S,\mu}$, $\nabla_T = d \ln T / d \ln p$, and $\nabla \mu = d \ln \mu / d \ln p$. The system is unstable for the overturning convection when $0 < R\rho^{-1} < 1$. The layered convection or turbulent diffusion occurs when $1 < R\rho^{-1} < (P_r + 1) / (P_r + \tau)$, where P_r is the Prandtl number and τ is the ratio of compositional to heat diffusivities. The system is stable when $R\rho^{-1} < 0$ or $(P_r + 1) / (P_r + \tau) < R\rho^{-1}$ (Rosenblum et al., 2011; Mirouh et al., 2012; Wood et al., 2013; Leconte & Chabrier, 2012).

We perform an evolutionary calculation of hot Jupiters with a self-consistent treatment of the convection regimes. We calculate the thermal evolution of the interior structures of hot Jupiters with the Henyey method (Kippenhahn et al., 1967). The method solves the equations of the one-dimensional interior structure in hydrostatic equilibrium. The convection regime is determined by the classification based on the density ratio $R\rho^{-1}$. We use the heat transport model for the overturning convection with the compositional gradient (Umezu & Nakakita, 1988). The transport model developed by Leconte & Chabrier (2012) is adapted for the layered convection.

We show that the impact of the compositional inhomogeneity is limited in the case of monotonic gradient of chemical composition, which is the same setup with Chabrier & Baraffe (2007). The reason for the limited effect is the absence of the layered convection. The convection regime is the overturning convection before ~ 1 Gyr. In the overturning convection regime, the efficient heat transport forces the temperature gradient to follow the neutrally stable state. Consequently, the super-adiabaticity is limited as $\nabla_T \sim \nabla_{ad} + \alpha \mu / \alpha_T \nabla \mu$. The layer forms only when 1 Gyr passes and the planet is already cooled, but the temperature gradient in this regime is limited as $\nabla_T < \nabla_{ad} + \alpha \mu / \alpha_T \nabla \mu$. Therefore, it is hard to explain the radius anomaly solely by this mechanism.

Keywords: exoplanet, hot Jupiter, thermal evolution, double-diffusive convection, layered convection

Planet Traps and Super-Earths: Implications for the Mass-Radius Diagram

HASEGAWA, Yasuhiro^{1*}

¹NAOJ

The discovery of a large number of super-Earths both by the radial velocity and by the transit has enabled a careful investigation of their composition that can provide fundamental constraints on their formation mechanisms. We present a statistical analysis for the population of planets that grow by the core accretion process at planet traps where rapid type I migration is halted. Evolutional histories of forming and migrating planets in evolving gas disks are computed theoretically in this model. We show statistically that the minimum mass of planets formed at planet traps via the core accretion scenario is about 5 Earth masses. These low-mass planets formed in our model are regarded as failed gas giants that contain a negligible or low mass atmosphere. Our results therefore imply that the composition of super-Earths may change from solid materials to gaseous/icy ones at about 5 Earth masses. Using a latest empirical mass-radius relationship, this transition value of planetary mass roughly corresponds to the recent estimate inferred from the Kepler data.

Tropopause of steam atmosphere and inner edge of habitable zone

ONISHI, Masanori^{1*}; HASHIMOTO, George²; KURAMOTO, Kiyoshi³; TAKAHASHI, Yoshiyuki O.¹; ISHIWATARI, Masaki³; TAKAHASHI, Yasuto³; HAYASHI, Yoshi-yuki¹

¹Department of Earth and Planetary Sciences, Kobe University, ²Department of Earth Sciences, Okayama University, ³Department of Cosmochemistry, Graduate School of Science, Hokkaido University

The inner edge of habitable zone is characterized by two specific limits. The first one is the runaway greenhouse limit at which the oceans evaporate entirely. The limit is estimated by the ratio of radiation limit to net incident solar flux. The second inner habitable zone boundary is water loss limit. If a planet would exist inner region of the loss limit, the planet could not retain water over a period of time sufficiently long to evolve life on the planet. The water loss limit is closely related to the tropopause temperature because the tropopause works as cold trap for water vapor.

Kasting 1988, Kopparapu et al., 2013 estimate two boundaries of inner edge of habitable zone for our solar system. The model pressure-temperature profiles consist of a moist pseudoadiabat extending from the surface up to an isothermal stratosphere. The stratosphere temperature is 200 K. Kasting et al., 1993 notes that this assumption (200 K stratosphere) has negligible effect on the runaway greenhouse limit, but may have a significant effect on the water loss limit. In this study, we calculate radiative transfer for the profiles consist of a moist pseudoadiabat extending from the surface up to top of atmosphere, and estimate tropopause temperature.

Our model pressure-temperature profiles consist of a moist pseudoadiabat (Nakajima et al., 1992) extending from the surface up to top of atmosphere. We assumed an Earth-mass planet with H₂O dominated atmosphere (H₂O and non-absorbed gas). Relative humidity is assumed to be unity. The surface temperature is varied from 250 to 400 K. The amount of non-absorbed gas is varied from 1e+3 to 1e+7 Pa. We use line data for water from the HITRAN2008 spectral database (Rothman et al., 2009), the continuum absorption from MT_CKD 2.5 continuum model (Mlawer et al., 2012) and ultraviolet absorption (Chan et al., 1993). Solar radiation is assumed as a black body radiation of 5800 K. A surface albedo is 0.2 in the wavenumber range from 3000 to 100000 cm⁻¹. A two-stream approximation (Toon et al., 1989) is used to calculate radiative transfer by line-by-line treatment with resolution of 0.01 cm⁻¹ wavelength in the range of 0 - 25000 cm⁻¹ and resolution of 10 cm⁻¹ in the range of 25000 - 100000 cm⁻¹. We estimate tropopause temperature from the heating rate profiles.

We estimate tropopause temperatures of around 150 K. The values are lower than that of previous studies are assumed. The lower temperature indicates that tropopause works stronger cold trap and the water loss limits locate nearer from the sun than that previously reported.

Keywords: steam atmosphere, radiative property, habitable zone, water loss limit

Lifetime and spectral evolution of a magma ocean with a steam atmosphere: its detectability by future direct imaging

HAMANO, Keiko^{1*} ; KAWAHARA, Hajime¹ ; ABE, Yutaka¹ ; ONISHI, Masanori² ; HASHIMOTO, George³

¹Department of Earth and Planetary Science, The University of Tokyo, ²Department of Earth and Planetary Sciences, Kobe University, ³Department of Earth Sciences, Okayama University

Theoretical studies predict that the final stage of terrestrial planet formation involves a series of giant impacts between proto-planets. In the aftermath of the last impact, the planets probably begin in a molten state. Detecting molten terrestrial planets in extrasolar systems is of great significance in testing the widely accepted view of their hot origins.

We present the thermal evolution and emergent spectra of solidifying terrestrial planets along with the formation of steam atmospheres. The lifetime of a magma ocean and its spectra through a steam atmosphere depends on the orbital distance of the planet from the host star. For a type-I planet, which is formed beyond a certain critical distance from the host star, the thermal emission declines on a timescale shorter than approximately 10^6 years. Therefore, young stars should be targets when searching for molten planets in this orbital region. In contrast, a type-II planet, which is formed inside the critical distance, will emit significant thermal radiation from near-infrared atmospheric windows during the entire lifetime of the magma ocean. The Ks and L bands will be favorable for future direct imaging because the planet-to-star contrasts of these bands are higher than approximately 10^{-7} - 10^{-8} . Our model predicts that, in the type-II orbital region, molten planets would be present over the main sequence of the G-type host star if the initial bulk content of water exceeds approximately 1 wt%.

Keywords: Magma ocean, Steam atmosphere, direct imaging, thermal emission spectrum

Formation and solubility of organic aerosols in the atmospheres of Titan and early Earth

TABATA, Haruhisa^{1*}; SEKINE, Yasuhito¹; SUGA, Hisami²; OGAWA, Nanako O.²; TAKANO, Yoshinori²; OHKOUCHI, Naohiko²

¹Department of Earth and Planetary Science, University of Tokyo, ²Department of Biogeochemistry, JAMSTEC

Titan, the largest moon of Saturn, might provide clues for the chemical evolution toward life in early Earth's atmosphere, as Titan has a thick atmosphere mainly composed of N₂ and CH₄ probably resembling that of early Earth. Titan is covered with thick haze layers of organic aerosols produced from chemical reactions initiated by the dissociation of N₂ and CH₄ caused by solar UV irradiations and Saturn's magnetospheric electrons bombardments. Previous studies performed laboratory experiments simulating Titan's organic chemistry by irradiating cold plasma to gas mixtures of N₂ and CH₄ in order to produce solid organic materials called tholin. Recent laboratory experiments also irradiated cold plasma or UV light onto gas mixtures of N₂-CH₄-CO₂-CO simulating early Earth's atmosphere. However, there are only few studies focusing on the mechanisms and formation processes of Titan and early Earth tholin. Moreover, organic aerosols formed in the atmospheres of Titan and early Earth would have undergone further reactions with liquid on the surface. Nevertheless, solubility of early Earth tholin to the organic solvent has not been studied.

We have conducted laboratory experiments simulating the formation of organic aerosols in the atmospheres of Titan and early Earth by irradiations of cold plasma onto gas mixtures of N₂-CH₄, N₂-CH₄-CO, or N₂-CH₄-CO₂. With the objective of revealing the processes of the tholin formation, mass spectrometry and emission spectroscopy were performed to identify the gas-phase reaction products. Chemical structures of the tholins were analyzed by infrared and UV-VIS spectroscopy. Production rates of tholin were examined by measuring the thickness of tholin with ellipsometry. We also performed solvent extraction of the tholin and analyzed the chemical structure by UV-VIS spectroscopy for the solvents.

Our experimental results show that the formation of Titan tholin from gas mixture of N₂-CH₄ occurs efficiently, compared with early Earth tholin formed from N₂-CH₄-CO or N₂-CH₄-CO₂. The formation rate of early Earth tholin decreases with CO₂ introduced in the initial gas mixture, whereas tholin forms efficiently from gas mixtures of N₂-CH₄-CO. Results of emission spectroscopy revealed that CN radicals are produced by plasma irradiations. Mass spectrometry of gas species demonstrated that HCN and cyanides, such as CH₃CN, are produced in the experiments in addition to hydrocarbons. These results suggest that the formation of Titan tholin is initiated by the production of CN radicals and subsequent cyanide formations. Regarding early Earth tholin, our results suggest the production of CN radicals as an important process for the tholin formation as well as Titan tholin. Though, the results from infrared spectroscopy suggests existence of C=O bonds in early Earth tholin. Thus, the production of CO and incorporation of oxygen into the tholin are also a significant process for the formation of early Earth tholin.

Our results of solvent extraction show that early Earth tholin dissolve effectively in polar solvents, such as methanol. We also found that early Earth tholin displays a dissolution to low-polar solvents, such as CH₂Cl₂, suggesting the existence of both non-polar and polar structures contained in early Earth tholin. Chemical structures that contain both hydrophilic and hydrophobic parts may have played an important role in the origination of bio-membrane structure (lipid bilayer). Also, our results from UV-VIS spectroscopy of CH₂Cl₂ solution of early Earth tholin display an absorption band typical to fused ring aromatic compounds or heterocyclic compounds including porphyrin. These results suggest that organic aerosols produced in the atmosphere of early Earth might have played a key role in the chemical evolution possibly by providing nitrogen-containing bio-related heterocyclic compounds as well as bipolar complex organics to pre-biotic oceans.

Keywords: Titan, early Earth, reducing atmosphere, organic aerosol, chemical evolution

Effects of Water Amount on the Surface Environment of Terrestrial Planets: High Pressure Ice and Carbon Cycle

NAKAYAMA, Akifumi^{1*} ; ABE, Yutaka¹

¹Department of Earth and Planetary, Graduate School of Sciences, The University of Tokyo

Terrestrial planets with several wt% of H₂O are theoretically predicted in habitable zone, where planet can sustain liquid water on its surface [Raymond et al., 2004]. Terrestrial planets in extrasolar planetary system are expected to have a large variety of water amount. In this study, we define two planetary modes; one is a planet that covered with ocean entirely (ocean planet) and the other is a planet that has oceans and lands (partial ocean planet), like Earth. We consider surface environment of terrestrial planets with various water amount focusing on CO₂, which is an important determining factor of the surface environment.

Carbon cycle stabilizes the surface temperature of the Earth. Weathering processes are the continental weathering and the seafloor weathering which occurs in oceanic crusts. On the Earth, the amount of atmospheric CO₂ (P_{CO_2}) is maintained at low level because of efficient continental weathering [Walker et al., 1981]. However, the efficiency of the continental weathering depends on the land fraction [Tajika and Matsui, 1993]. On the other hand, the seafloor weathering is poorly constrained; several models that depend on pH [Caldeira, 1995] or hydrothermal circulation [Sleep and Zahnle, 2001] or seafloor temperature [Brady and Gislason, 1997] have been proposed.

On the ocean planets, seafloor weathering is important because the continental weathering does not work. The increase of water amount has two effects in P_{CO_2} ; one is the enhancement of the seafloor weathering due to temperature rise and the other is the increase of the degassing rate of CO₂, caused by the increase of the total amount of CO₂. P_{CO_2} in the ocean planets is determined by the competition between both processes. In addition, a planet with large water amount may form high-pressure (HP) ice on the seafloor [Leger et al., 2004]. In such a case, any weathering processes will not work and P_{CO_2} will be extremely high. On the other hand, high surface temperature may prevent it.

In this study, we focus on the carbon cycle and HP ice and aim to clarify the relationship between the water amount on surface P_{CO_2} . In particular, we discuss the difference in P_{CO_2} between partial ocean and ocean planets.

We built a carbon cycle model by adding the seafloor weathering to the Earth's carbon cycle model by Tajika and Matsui [1992]. Degassing rate is depended on the total amount of carbon. We assume carbon is also supplied with water. We discuss the dependence on the land fraction in partial ocean planets or the water amount in ocean planets. We examined the P_{CO_2} in equilibrium state in which degassing and regassing are balanced. We also consider effect of HP ice on carbon cycle.

On the partial ocean planets, we found that continental weathering is the dominant weathering process when the land fraction is 0.1 or more. Even if the degassing rate is five times as large as the current value of the Earth, P_{CO_2} on the partial ocean planets is lower than $30P^*$ (P^* is atmospheric CO₂ level in the current Earth). On ocean planets, we found that the increase of degassing rate surpasses the enhancement of the seafloor weathering efficiency upon the increase of water amount. Even if seafloor weathering works most efficiently, P_{CO_2} increases with increase of water amount and P_{CO_2} becomes about $1000P^*$. In the case that HP ice is formed on the seafloor, a cycle of HP ice formation (the disappearance of the seafloor weathering) and disappearance (the resume of the seafloor weathering) is expected to occur. In cases that water amount is larger than 120 Earth's ocean mass, HP ice is formed and P_{CO_2} is expected to rapidly increase with increase of water amount. Our results suggest that P_{CO_2} on an ocean planet is significantly different from that of partial ocean planets, on which the continental weathering works efficiently. Our results also suggest that the process of determining P_{CO_2} changes with the water amount, and surface environment varies greatly with it.

Keywords: carbon cycle, seafloor weathering, high-pressure ice, carbon dioxide, terrestrial planet, extrasolar planet

The duration of habitable condition for large and small Earth-like planets

KADOYA, Shintaro^{1*} ; TAJIKA, Eiichi²

¹Earth and Planetary Sci., Univ. of Tokyo, ²Complexity Sci. & Eng., Univ. of Tokyo

The orbital condition for the Earth-like planets which may have liquid water on its surface is known as the habitable zone (e.g., Kasting et al., 1993; Kopparapu et al., 2013). However, the condition for the Earth-like planets which can maintain the warm and wet climate through the evolution may be different from that for the habitable zone. The climate of the Earth-like planets would actually depend on the CO₂ degassing rate via volcanism because the amount of the atmospheric CO₂ is controlled by the carbonate-silicate geochemical cycle (Kadoya & Tajika, 2014, ApJ, 790:107). The CO₂ degassing rate decreases with time owing to decrease in mantle temperature and attenuation of volcanic activity (Tajika & Matsui, 1992, EPSL, 113). The thermal evolution of the planets should, however, depend on the planetary mass.

In this study, we apply a parameterized convection model to the thermal evolution of the Earth-like planet with different masses and with plate-tectonics in order to estimate the evolution of average mantle temperature, seafloor spreading rate, melt generation depth, melt production rate, and the CO₂ degassing rate for the planets. The results are compared with the climate mode diagram for the Earth-like planets proposed by Kadoya & Tajika (2014), and also, the evolutions of the climate of the Earth-like planet are discussed.

The average mantle temperature monotonically decreases with time when an initial average mantle temperature is higher than 3000 K. As expected, the average mantle temperatures of large planets cool more slowly than that of small planets do. However, the difference between the mantle temperatures of the planets is smaller than 100 K, which is consistent with the recent work (e.g., Schaefer & Sasselov, 2015). The seafloor spreading rate is larger on large planets than on small planets because the heat flow is higher on large planets than on small planets. On the other hand, the melt generation depth of large planets is smaller than that of small planets owing to the difference in the surface gravity. The net result of the melt generation rate is larger on large planets than on small planets although the difference is smaller than those of the seafloor spreading rate and the melt generation depth. In addition, because large planets have a larger surface area than small planets, the CO₂ uptake rate via silicate weathering on large planet is larger than that on small planets when the temperature distribution is the same. As a result, the climate evolutions of large and small planets are almost the same as long as the areal ratio of continents and oceans is the same.

Keywords: exoplanet, habitable zone

A new climate instability that triggers the runaway greenhouse in a 3-dimensional heterogeneous world.

ABE, Yutaka^{1*} ; NITTA, Akira¹ ; ABE-OUCHI, Ayako² ; O'ISHI, Ryouta² ; TAKAO, Yuya³

¹School of Science, University of Tokyo, ²Atmosphere and Ocean Research Institute, University of Tokyo, ³Center for Public Affairs and Communications, Tokyo Institute of Technology

The onset condition of the runaway greenhouse is considered that the atmosphere takes in more incoming solar radiation than a "runaway threshold." The runaway threshold is important because it defines the absolute inner limit of the habitable zone. Most of previous studies on the runaway threshold used one-dimensional radiative-convective equilibrium model and considered the atmospheric state where the ocean cannot exist in an equilibrium state. Such studies indicated that the runaway threshold is the "radiation limits," which is an asymptotic value or an upper limit of the planetary radiation (Nakajima et al., 1992,).

Recently, the runaway threshold of planets with heterogeneous surface water distribution has been investigated using 3-dimensional dynamic models (Abe et al., 2011; Leconte et al., 2013; Nitta et al., in preparation). The threshold strongly depends on the surface water distribution and it can be quite different from the radiation limit. Therefore, we have to understand the controlling mechanism of the runaway threshold in a 3-dimensional world.

Here, we report a new climate instability that triggers the runaway greenhouse based upon the analysis of GCM results and the linear stability analysis of a simplified model. The instability requires horizontal transport of heat and water vapor, thus it does not appear in one-dimensional world. On the other hand, surprising enough, this instability does not require the radiation limit. Namely, the instability is not directly related to the asymptotic value or the upper limit of the planetary radiation. This result suggests that the onset of the runaway greenhouse in 3-dimensional heterogeneous world may not be understood in terms of the simple radiation limit.

Keywords: runaway greenhouse, habitable zone, radiation limit, climate instability

The vigor and the regime diagram of thermal convection in the mantle of massive super-Earths

MIYAGOSHI, Takehiro^{1*} ; KAMEYAMA, Masanori² ; OGAWA, Masaki³

¹Jamstec, ²Ehime University, ³University of Tokyo

Understanding thermal convection in the mantle of super-Earths is a key to clarifying their thermal history and habitability. In massive super-Earths, the strong adiabatic compression influences thermal convection in the mantle in contrast to the Earth's one. In this paper, we present numerical models of thermal convection in massive (ten times the Earth's mass) super-Earths calculated at the relevant adiabatic compression effect and various values of Rayleigh number Ra and temperature-dependent viscosity contrast r .

Strong effects of adiabatic compression reduce hot plume activity significantly, while keeping cold plume activity high. The effects on hot plumes become more prominent as r increases, because the lithosphere becomes thicker as r increases and the potential temperature of the isothermal core increases. This results in decreasing difference of potential temperature between hot plumes and surround material, thus in decreasing buoyancy force of hot plumes.

We also studied the convective regime diagram on the plane of Ra and r . The threshold value of r for transition to the stagnant lid regime from small viscosity contrast regime increases as Ra increases in super-Earths in contrast to the diagram of the earlier Boussinesq model [Kameyama and Ogawa, 2000]. At high Ra relevant to massive super-Earths, the threshold value is larger than that expected in the Earth. To understand the reason why the threshold value of r increases as Ra increases, we present the viscosity contrast between the surface of the planet and the bottom of the lithosphere $reff$. In contrast to the increasing the threshold value of r , the $reff$ is constant even the Rayleigh number increases. Thus, the $reff$ is more relevant to transition to the stagnant lid regime rather than the viscosity contrast r in the whole mantle.

We also found that the Nusselt number Nu , which is the efficiency of heat transport by thermal convection, is considerably reduced compared with the earlier Boussinesq model. At $Ra=10^{10}$ and $r=10^7$, the Nu is only 2.7 and 14% of the value expected from the earlier Boussinesq model. The thickness of the lithosphere is about 30% of the depth of the whole mantle. From systematic numerical simulation, Nu is fitted as a function of Ra and r . The power index on Ra is 0.27. This value is somewhat smaller than that in the earlier Boussinesq model (0.31) [Christensen, 1984].

The thick lithosphere shown in our model implies that plate tectonics is difficult to operate in super-Earths. However, the high threshold value in r for regime change suggests that the lithosphere moves in a way different from plate tectonics. Thermal convection may be in the small viscosity contrast regime in super-Earths and the surface may be fully involved in the convective current.

Keywords: super-Earths, mantle, thermal convection, compressible fluid, stagnant lid, numerical simulations

Tidal resonance in icy satellites with subsurface oceans

KAMATA, Shunichi^{1*} ; MATSUYAMA, Isamu² ; NIMMO, Francis³

¹Hokkaido Univ., ²LPL/Univ. Arizona, ³UC Santa Cruz

Tidal dissipation is a major heat source for the icy satellites of the giant planets. Several icy satellites likely possess a subsurface ocean underneath an ice shell. Previous studies of tidal dissipation on icy satellites, however, have either assumed a static ocean, or ignored the effect of an ice lid on subsurface ocean dynamics. In this study, we extend the formulation for tidal deformation based on the viscoelasto-gravitational theory to incorporate inertial effects and obtain a comprehensive equation system that can be applied to a model with a dynamic ocean overlain by an ice lid. Although ocean dynamics are treated in a simplified fashion, we find a resonant configuration when the phase velocity of gravity waves approaches the orbital velocity. The enhanced deformation near the resonant configuration would lead to significantly enhanced tidal heating in the solid lid. A static ocean formulation would give an accurate result only if the ocean thickness is larger than the resonant thickness by a factor of about one hundred. The resonant configuration strongly depends on properties of the shell, demonstrating the importance of the presence of a shell on tidal dissipation.

Keywords: Icy satellites, Subsurface ocean, Tidal response, Resonance

The temporal evolution of rheological structure of Martian interior

AZUMA, Shintaro^{1*} ; KATAYAMA, Ikuo¹

¹Hiroshima University

Change of the rheological structure significantly influences the Martian evolution, which might results in the different tectonics operated in between Mars and Earth. Here we show the evolution of rheological structure of Martian lowlands (North Pole) and highlands (Solis Planum) under wet and dry conditions. The thermal state of the past and present planetary interior can be calculated from surface heat flow and the present-day abundance of the radioactive isotopes ²³⁸U, ²³⁵U, ²³²Th, and ⁴⁰K [Turcotte and Schubert, 2002]. Rheological structure can be inferred from flow laws that indicate the strength of solids, which is dependent on strain rate, temperature, and chemical composition [Frost and Ashby, 1982; Karato and Jung, 2003]. Power-law creep is generally used to infer rheological structure and heat flow [Grott and Breuer, 2008; Ruiz et al., 2008; Grott and Breuer, 2010], and this type of flow law is commonly applied to high-temperature creep. However, the Peierls mechanism becomes dominant at low temperatures and high stresses [Tsen and Carter, 1987]. In this mechanism, strain rate is exponentially proportional to applied stress. In this study, the Martian rheological structure is determined not only from Power-law creep but also from the Peierls mechanism and diffusion creep. The rheological structure of Mars determined in this study indicates that shallow deformation on Mars is mostly controlled by the Peierls mechanism, and that application of power-law creep on its own leads to an overestimation of lithospheric strength. Our results show that the presence of water would have delayed increases in elastic and lithospheric thickness on Mars, in addition to decreasing the elastic thickness through reduced rock strength and the production of incompetent crust and mantle. The lithospheric strength of the North Pole for a wet rheology at 4 Ga might have had a moderate strength of 200-300 MPa. Likewise, the lithospheric strength of the Solis Planum at 2.4 Ga was probably moderate, indicating that the rheological structures of the North Pole at 4 Ga and of Solis Planum at 2.4 Ga under wet conditions might have allowed the formation of plate boundaries, which are necessary for the initiation of plate tectonics.

Keywords: Mars, Rheological structure, Plate tectonics, Lithosphere, Peierls mechanism, Temporal evolution

Development of an in-situ dating package for lunar/Mars missions

CHO, Yuichiro^{1*} ; SHIBASAKI, Kazuo¹ ; UMEYAMA, Misako¹ ; OISHI, Takahiro³ ; KAMEDA, Shingo¹ ; MIURA N., Yayoi² ; YOSHIOKA, Kazuo³ ; SAITO, Yoshifumi³ ; YOKOTA, Shoichiro³ ; KASAHARA, Satoshi³ ; YOSHIMITSU, Tetsuo³ ; OKAZAKI, Ryuji⁴ ; OHTAKE, Makiko³ ; MOROTA, Tomokatsu⁵ ; KOGA, Sumire⁷ ; SUGITA, Seiji⁶

¹Rikkyo University, ²Earthquake Research Institute, University of Tokyo, ³ISAS, ⁴Kyushu University, ⁵Nagoya University, ⁶Dept. Earth and Planetary Science, University of Tokyo, ⁷Dept. Complexity Science and Engineering, University of Tokyo

Age data of geologic records on the Moon and Mars will significantly improve our understanding of their evolution. We have been developing an in-situ K-Ar dating instrument and conducted a series of experiments to demonstrate its principle. In this presentation, we report the recent progress in the engineering aspect of our instrument.

First, we have established the design of our instrument package and the procedure of age measurements. Second, we have designed a sample handling system using parallel link motion. Third, we conducted blank measurements using the noble-gas analysis system we built previously, in order to investigate the capability of O-rings as seal materials. We used Viton and Nexus-SLT O-rings instead of metal gaskets. Our results indicate that a metal seal can be replaced with sufficiently baked Viton O-rings in the lunar environment because there is no atmosphere permeating through the O-ring. Our experimental results also indicate that under the pressure of Martian atmosphere (i.e., 6 hPa), a sufficiently low blank level can be achieved by using a double O-ring evacuating system. Above-described developments enhance the technical feasibility of our in-situ geochronology instrument.

Verification of in-situ K-Ar dating using LIBS

SHIBASAKI, Kazuo^{1*}; OKUMURA, Yu¹; CHO, Yuichiro¹; KAMEDA, Shingo¹; MIBE, Kenji²; MIURA, Yayoi N.²; SUGITA, Seiji²

¹Rikkyo University, ²The University of Tokyo

Knowing the age of planetary surfaces is important. In recent years, *in-situ* dating techniques without sample-return missions have been developed. *In-situ* dating conducted by NASA's Curiosity rover on Mars is the only example of such measurements on another planet. Curiosity obtained the K concentration with an Alpha Particle X-ray Spectrometer (APXS) and the Ar concentration with a quadrupole mass spectrometer (QMS), and obtained the K-Ar age of a mudstone at the Gale crater. However, since this system is very complicated, a large rover is needed for operation. Therefore, we investigated conducting both K and Ar measurements using only Laser-Induced Breakdown Spectroscopy (LIBS). Since our method requires only one detection, the instrument package can be more compact and lighter compared with NASA's method. Furthermore, LIBS enables remote and rapid measurements. However, Ar gas contained in a rock has been never detected with LIBS.

In this study, we conduct verification experiments for detection of Ar in rocks using LIBS.

Temperature and electron density of LIBS plasma under atmospheric pressure are expected to be 1 eV (11600 K) and 10^{17} cm⁻³, respectively. We calculated the Ar line intensity at these values using the Saha equation and found that the neutral emission lines at 104.8 nm and 106.7 nm are the strongest ones. We then conducted spectroscopic experiments in a vacuum ultraviolet range (i.e., 10-200 nm). We used a standard basalt sample with known chemical composition (JB-1a) and a sample with enhanced Ar concentration (Ar concentration is 0.1 cc/g). We used an Nd:YAG laser ($\lambda=1064$ nm; pulse width 5-7 ns; pulse energy 50 mJ). The emissions from laser-induced plasma is diffracted by concave diffraction grating. The detector is MCP with a phosphor screen. We captured the spectra images on the phosphor screen with a CCD camera.

In a preliminary experiment using pure silicon as a sample, we detected the Si⁽³⁺⁾ emission line at 106.7 nm. This suggests that the temperature of plasma is higher than expected, because the Si⁽³⁺⁾ emission line requires high excitation energy. Considering the high temperature, and because Ar is thought to be ionized at such a high temperature, we then tried to detect the Ar⁽⁴⁺⁾ emission line at 83.5 nm because this line had higher detectability than the neutral emission lines. However, we found that an O⁽²⁺⁾ emission line at 83.4 nm interfered with the Ar⁽⁴⁺⁾ line. In our study, we detected a number of multiply charged ion emission lines and found that the Si⁽³⁺⁾ emission line at 106.7 nm and O⁽²⁺⁾ emission line at 83.4 nm overlapped with the Ar emission lines. Since the plasma temperature drops rapidly with time, our results indicate that a gate pulse to detector is effective for removing the emission lines of multiply charged ions.

Keywords: LIBS, in-situ dating, K-Ar method

An outline of the road map of planetary sciences and solar system sciences

KURAMOTO, Kiyoshi¹ ; ARAI, Tomoko² ; KOBAYASHI, Naoki³ ; SUGITA, Seiji⁴ ; TACHIBANA, Shogo¹ ;
TERADA, Naoki⁵ ; NAMIKI, Noriyuki^{6*} ; MATSUMOTO, Koji⁶ ; WATANABE, Sei-ichiro⁷

¹Graduate School of Sciences/Hokkaido University, ²PERC/Chiba Institute of Technology, ³ISAS/JAXA, ⁴Graduate School of Science/The University of Tokyo, ⁵Graduate School of Science/Tohoku University, ⁶RISE/NAOJ, ⁷Graduate School of Science/Nagoya University

Answering to the request from ISAS/JAXA, the president and his advisory committee of Japanese Society for Planetary Science (JSPS) submitted a road map for the next 20 years of the Solar System Exploration of Japan on 2015 February 2. Needless to say, this road map is of particular importance for the future of planetary science community. Nevertheless, the short period of the preparation prevented a deep argument among the planetary science community on this road map. As the committee members, the authors realize keenly the necessity of continuing discussion on this road map and decided to give a talk at the JpGU meeting to attract attention of every community member on this subject. The proposed road map and the processes until finalizing the document are explained by the committee to start further arguments with anyone who concerns about the future of the solar system exploration.

Keywords: road map, future plan, solar system exploration, planetary exploration

Fracture process inferred from fragment shape in impact disruption

KADONO, Toshihiko^{1*} ; TANIGAWA, Takayuki¹ ; MIZUTANI, Hitoshi²

¹University of Occupational and Environmental Health, ²Newton Press

The results of the previous impact experiments show that the shape of the fragments, characterized by the triaxial dimensions a , b , and c , ($a \geq b \geq c$), behaves in a very regular way (e.g., Fujiwara et al. 1989). In widely different experimental conditions, the axial ratios, b/a and c/a , have distributions peaked at about each mean value, ~ 0.7 and ~ 0.5 , respectively, and flattened (i.e., small c/a) fragments are almost absence.

We find that, if the distribution of the shape parameters, (b/a , c/a), is homogeneous, and there is no fragment at $c/a < k$, where k is a constant ($0 < k < 1$; in Fujiwara et al. (1978) k was ~ 0.2), the averages of the shape parameters, (0.7, 0.5) can be realized. Then, we discuss the fracture processes to represent the homogeneous distribution in the shape parameters. The expected dominant fracture process in impact fragmentation is reported.

Fujiwara, A., et al., Nature 272, 602-603, 1978.

Fujiwara, A., et al., in Asteroids II, pp. 240-265, 1989.

Keywords: impact, disruption, fragment shape, fracture process

Experimental study on collisional destruction of iron bodies: Temperature dependence

OGAWA, Ryo^{1*} ; NAKAMURA, Akiko¹

¹Graduate School of Science,kobe University

Introduction: Iron meteorites are composed of iron-nickel alloys and most of them have unique crystalline structures known as Widmanstätten patterns. They undergo a transition from ductile to brittle behavior as the temperature is lowered. It is thought that they may have been derived originally from the cores of their parent bodies and so they may tell us the history of planetary formation. If the collisional destruction of cores of parent bodies occurred, fragments of them should be scattered as iron asteroids, but they have not been discovered yet. M-type asteroids may be iron asteroids but it is found that some of them have low density, and might be rubble-piles. We performed impact experiments and examined the temperature dependence of degree of disruption and fragment velocity in order to collect basic data for studying the possibility of formation of iron-rubble-pile asteroids.

Experimental method: We performed impact experiments using two different guns. Impact experiments with velocities of 0.6-1.2 km/s were performed using a powder gun at Kobe University and with velocities of 6.8-7.3 km/s were performed using a two-stage light-gas gun at the Institute of Space and Astronautical Science (ISAS). The projectiles were cylinders 15 mm in diameter machined from stainless steel or nylon spheres 7 mm in diameter. The targets were blocks of Gibeon iron meteorite or cylinders 25 mm and 35 mm in diameter machined from SS400 steel. We used room-temperature targets in the experiments using the two-stage light-gas gun, while we used room-temperature (298K) and low temperature (170-150K) targets in the powder gun-experiments. We compared the velocity distribution of fragments, fragment mass distribution and relationship between energy density and largest fragment mass fraction in low temperature and room temperature to examine the temperature dependence. We measured velocities of fragments using a high-speed camera. Additionally, we performed impact experiments using two targets with different aspect ratios (0.37 and 1) to examine the effect of target shape.

Results: We measured fragments with velocity 20-900 m/s and found that most fragments have velocities lower than the escape velocity of Psyche, i.e., 130 m/s. Temperature dependence is seen in the fragment mass distribution and the relationship between energy density and largest fragment mass fraction. The total mass fraction of SS400 steel fragments with mass less than 1 % of the initial mass accounted for 2.4-25 % of the initial mass at low temperature, whereas 0.12-18 % of the initial mass at room temperature. Energy density for destruction of targets with aspect ratio 0.37 is lower at low temperature than room temperature, which is not seen in previous studies.

Keywords: iron meteorites, impact, rubble-pile

Porosity of Granular Surface of Small Bodies - Relationship between Pressure and Porosity

OMURA, Tomomi^{1*} ; KIUCHI, Masato¹ ; GUETTLER, Carsten² ; NAKAMURA, Akiko¹

¹Graduate School of Science, Kobe University, ²Max-Planck-Institute for Solar System Research

The Moon and many asteroids have regolith on the surface. Regolith can have various porosities and if we compress powder bed that has porosity, porosity is expected to decrease. Revealing the relationship between pressure and change in porosity makes it possible to estimate penetration depth of interplanetary dust particles or meteorites, and lander on asteroids. Porosity of planetesimals formed of dust aggregates is theoretically expected to 90 % (Kataoka et al., 2013). On the other hand, laboratory experiments show that surface of target constructed by such fluffy dust aggregates is compressed when impacted by sieved dust aggregates (Meisner et al., 2012). It is possible that porosity of planetesimals can be changed by impacts between planetesimals. Revealing their relationship is useful to estimate aggregate's porosity during the evolutionary process toward planets.

First, it is necessary to determine porosity before compression. In this work, we focus on regolith on asteroids, i.e. granular bed accumulated under microgravity conditions. Porosity is determined by configuration of particles. Factors affecting regolith porosity are particle diameter, particle shape, interparticle force, and gravity. An empirical formula that include force ratio between interparticle force and gravity is presented (Yu et al., 2003; Kiuchi and Nakamura, 2014). However, this empirical formula is obtained by measurements under 1 G, so it is necessary to check if this formula can work under microgravity. Additionally, particle size distribution is not included in this formula. Regolith particle is not monodisperse because regolith is made up of impact fragments. So it is necessary to take effect of particle size distribution into account. Size distribution of impact fragments is usually represented as power-law. A geometric model has been proposed to estimate the porosity of granular bed that has close packing state (e.g. made by tapping) constructed by particles having power-law size distribution (Suzuki et al., 2001). However, porosity of loose packing state doesn't agree with the value predicted by the model. More studies for relationship between porosity of loose packing state and particle size distribution are needed to estimate initial porosity of regolith after deposition.

Second, we consider cases of impact or landing, i.e., when pressure is applied to regolith.

In this study, we conduct compression experiment of silica sand 1-3, of similar shape and different size distributions (median diameter is 13 μm , 24 μm , and 73 μm , respectively) fly ash (4.5 μm), fused alumina particles (5.3 μm), and basalt fragments smaller than 210 μm prepared by an impact experiment (29 μm) (hereafter called "basalt") using a centrifuge and compression testing machine.

We sieved them into a cylindrical container of diameter 5.8 cm and depth 3.3 cm (for basalt, diameter 2.7 cm and depth 1.4 cm) and the top part of the bed over the height of the container was leveled off. Silica sand 2 and basalt samples are resemble in median diameter, but porosities before compression are different, 58 % and 52 %, respectively. That means basalt has lower porosity. Power indices of cumulative volume fraction versus particle size are 0.53 and 0.78, respectively, so we obtained similar result with Suzuki et al. (2001): in the cases of loose packing state, porosity decreases with increase of the power index. We applied 1-18 G by the centrifuge or up to 106 Pa by the compression testing machine on the sample and determined porosity after compression from the sample volume obtained by bed height or displacement by compression.

In this presentation, we make a comparison between our result and existing powder compaction equations. In addition, we discuss about change in porosity by pressure and change in compressive strength by porosity in relation with particle size distribution.

Keywords: planetesimals, asteroids, porosity, powder and granular material

Impact experiments in viscous fluid: Implications to crater formation and viscous relaxation on cometary nuclei

ABE, Hitomi^{1*}; ARAKAWA, Masahiko²; YASUI, Minami²

¹Graduate School of Engineering, Yokohama National University, ²Graduate School of Science, Kobe University

Introduction: A cometary nucleus is supposed to be composed of rocks, ices and organic matters, and comets could be one of the most primordial bodies in the solar system because cometary nuclei would have never experienced high thermal metamorphism to evaporate water ice from the interior since their formation. Thus, it is very interesting to explore the internal structure, but the direct observation of the interior is quite difficult. While the morphology of the impact craters on the surface of cometary nucleus is expected to reflect the internal structure, therefore, it is important to study the formation process of impact craters on the surface simulating the comet nuclei in order to clarify the internal structure of cometary nuclei. Several circular depressions on the surface of cometary nuclei were found by the space craft such as Stardust and Rosetta, but their morphology was quite different from those on the rocky bodies such as the Moon because of the viscosity of refractory organic matters constructing the surface layer. In this study, we carried out impact experiments on viscous fluids and examined the effect of viscosity on the crater volume.

Experimental methods: We did impact experiments by using the one-stage vertical He-gas gun at Kobe University. We prepared a target by mixing glucose syrup with water, and the viscosity was controlled from 10^{-3} to 47 Pas. A projectile was a disk-shaped agar with the diameter of 10 mm and the thickness of 5 mm. We chose the agar as a projectile material because we'd like to study the effect of projectile destruction at impact. The projectile velocity was a constant of 65 ± 15 m/s, and the impact experiments were carried out under the air pressure. The cratering phenomena were observed by a high-speed camera, and we analyzed the crater depth changing with the time and the crater maximum diameter.

Result: We measured the time change of the crater depth and diameter by using the video images, and examined the effect of viscosity on these sizes. First, we found that the crater depth increased with the increase of time, and it became the maximum at a certain time. So we calculated the crater volume by using the maximum depth and the diameter measured at this time. In this study, we examined the relationship between the non-dimensional crater volume, $\pi^{1*} = (V\rho/m) \cdot (1.61gD_p/u^2)^a$ (V : crater volume, ρ : target density, g : gravity, D_p : target diameter, u : velocity, a : constant), and the non-dimensional viscosity, $\pi^{2*} = (\eta/(\rho D_p u)) \cdot (1.61gD_p/u^2)^{(a-1)/2}$ (η : viscosity). As a result, the π^{1*} became constant, irrespective of the viscosity at small π^{2*} (gravity regime), while the π^{1*} decreased with the increase of viscosity at large π^{2*} (viscous regime). Fink et al. (1984) showed the similar behavior, so we can say that this trend did not depend on the impact velocity. But our π^{1*} was relatively smaller than that of previous works and the power of the fitting line by using the power equation in viscous regime was larger than that of previous work.

Next, we calculated the relaxation time as the duration from the time when the crater depth became the maximum to the time when the depth becomes $1/e$ times as large as the maximum. As the result, the relaxation time was larger with the increase of the viscosity. We calculated the theoretical relaxation time by using the equation of $t_R \cong 8\eta/(\rho g D_c)$ (D_c : crater maximum diameter), and compared this theoretical values with our results. As a result, our experimental results were larger than the theoretical values as the viscosity became larger.

Keywords: impact crater, cometary nuclei, viscosity, relaxation time

Tensile, crushing, and impact strength and their relationships for chondrules and other rock samples

SHIGAKI, Sae^{1*} ; NAKAMURA, Akiko¹

¹Graduate School of Science, Kobe University

There are different scenarios for chondrule formation. Chondrules are thought to be captured into chondrites after their formation, then underwent collisional and thermal evolutions. Beitz et al. (2013) studied the relationship between pressure and porosity based on impact compression experiments of simulated chondrite samples. They showed that the maximum pressure which chondrite parent bodies experienced can be estimated from the tensile strength of chondrules and the fraction of intact chondrules. However, the tensile strength of chondrules is not known. Therefore we started to estimate the tensile strength of chondrules in order to discuss the maximum pressure chondrite parent bodies experienced.

The strength measurable for chondrules is crushing strength of spherical samples. Generally, tensile strength is measured using shaped samples, while it is difficult to shape chondrules. In stead, we estimate the tensile strength from the crushing strength of chondrules assuming that the relationship between these strengths of other samples can be applied to those of chondrules.

Static compression experiments of about 30 chondrules showed that the crushing strength of chondrules is around 8 MPa (Shigaki & Nakamura, Fall meeting of The Japanese Society for Planetary Sciences 2014). It is shown from the measurement of the strength of dunite samples that crushing strength and tensile strength are almost equivalent. Furthermore, we tried to estimate the crushing strength from impact strength. Using the results of impact disruption experiments of chondrules (Ueda et al., 2001), we found that the crushing strength of chondrules might possibly be stronger (~30MPa). The inconsistency of the values of crushing strength can be due to different relationships between these strengths for different silicate materials.

In this study, we employed more variety of rock samples to examine their tensile, crushing, and impact strengths and their relationships, in order to obtain more reliable tensile strength of chondrules. We prepared disk and spherical samples of dunite, basalt, Berea sandstone, and tuffaceous sandstone. While chondrules were removed from Allende (CV3) specimens in the previous experiment using tweezers and files, we separated them from matrix by means of Freeze-thaw method. We will perform impact experiments of chondrules onto a stainless steel plate to obtain the impact strength of chondrules.

In this presentation, we will introduce our results of all samples used so far and discuss the tensile strength of chondrules estimated from the relationships of these strengths for the different silicate samples.

Keywords: chondrites, chondrules

The inclination evolutions of protoplanets through giant impacts

MATSUMOTO, Yuji^{1*} ; NAGASAWA, Makiko² ; IDA, Shigeru²

¹NAOJ, ²Tokyo Institute of Technology

The Kepler mission has reported over 3500 planetary candidates (e.g., Batalha et al., 2014).

There are 899 transiting planet candidates in 365 multiple-planet systems, and 333 systems are only composed by 818 ungiant candidates, whose radii are smaller than 6 Earth radius, and which are composed by Neptunes and super-Earth.

When multiple planets are detected by the transit method, the mutual inclinations can be estimated by the ratio of transit duration times.

Fabrycky et al. (2014) suggested that the typical mutual inclination between Kepler candidates in multiple-planet systems lies in 1.0 degree - 2.2 degree.

Inclinations of protoplanets are excited by the mutual scatterings between them.

It is expected that protoplanets can excite the inclinations up to the half values given by their escape velocities.

The excited inclination is estimated as $i_{esc} = 5.4$ degree for a 10 Earth mass planet at 0.1 AU.

The small inclinations of observed ungiants suggest that if they are formed in-situ accretion, some inclination damping mechanism is working.

Since the eccentricities of the merged protoplanets are damped through giant impacts between protoplanets, as pointed out by our previous study, the inclinations is expected to be damped by the giant impacts.

On the other hand, for a Earth mass planet at 1 AU, $i_{esc} = 8.6$ degree.

The resultant planets from N-body simulations in the giant impact stage normally have $i = 3$ degree without any damping forces (e.g., Kokubo et al. 2006).

Ths smaller inclinations of calculated planets also suggest that inclinations are damped through the giant impact.

We investigate inclination evolutions through the collisions in the giant impact stage by N-body simulations.

We find that the inclination of the merger body is smaller than the larger inclination of the colliding two protoplanets.

The inclination after a collision is expressed as the function of the mutual inclination and the angular momenta.

Our N-body simulations suggest that the inclinations of observed ungiant planets can be reproduced by the in-situ accretion of planets in the gas-free environment.

Keywords: planetary accretion, giant impact phase, inclination

The formation probability of the binary planet

ARAKAWA, Sota^{1*} ; NAGASAWA, Makiko¹ ; NAKAMOTO, Taishi¹

¹Tokyo institute of technology

Binary planet is a system in which two planets revolve around a central star while rotating around each other. In the case of gaseous planets, a planet can capture the other planet by the tidal force when they closely approach during the planet scattering process. We study the closest distance between the planets during the scattering phase and determine the probability of binary planets formation.

It is known that the amount of energy dissipated by dynamical tides significantly depends on the distance between the planets. For two planets to be captured as a binary planet, it is necessary that the planets approach within several times of their physical radii. How multiple planets approach can be calculated only by mutual gravitational interactions, regardless of the details of the tidal model. In addition, the encounters of planets do not occur continuously unlike the encounter of the central star and the planet. Previous studies suggest that the formation of binary planets takes place immediately after the start of the orbital instabilities. We stop our calculations by 10000 Keplerian orbits, but perform 10000 simulations, which allow the statistical discussion. We compare Jacobi integral and the tidal energy to be dissipated at their closest encounter.

Results of our simple approach are almost consistent with the previous study, which performed orbital calculations including tidal dissipations (Ochiai et al. 2014). We find that the probability of binary planet formation was about 10%, independent of the semi-major axis. We vary the strength of tides as a parameter. We find that when the tidal dissipation is four times stronger, the formation probability of the binary planet becomes approximately two times larger. The probability of formation becomes 1/4 when the tides are 1/4.

Keywords: binary planet, N-body simulation

Transmission spectrum models of exoplanet atmospheres with haze: Effects of growth and settling of haze particles

KAWASHIMA, Yui^{1*} ; IKOMA, Masahiro¹

¹The University of Tokyo

Since the first discovery of an exoplanet in 1995, detection of more than 1500 exoplanets has been reported. Recently, in addition to detection, multi-wavelength transit observations have been done to characterize detected exoplanets. From a decline in apparent stellar brightness due to a planetary transit, we can measure the planetary radius. Also, the observed wavelength-dependent radius (which is often called the transmission spectrum) provides the information of absorption and scattering of stellar light by molecules in the planetary atmosphere. Thus, the composition of the planetary atmosphere can be constrained by comparison between the observational and theoretical transmission spectra. The constraint on atmospheric composition is expected to give an important clue to the origin of the planet.

Until today, transmission spectra of 20 exoplanets have been obtained. Some of the recent observations detected flat or featureless spectra, inferring the existence of particles such as hazes floating in the atmosphere. This means the existence of hazes would obscure the predicted spectral features of molecular absorption, making it difficult to prove its atmospheric composition. Also, the transmission spectra seem to be somewhat diverse. Some contain the Rayleigh-slope feature in the visible, some show molecular and atomic features in the near-IR. These observational facts raise questions such as how common hazy atmospheres are beyond the solar system, how diverse transmission spectra of hazy atmospheres are, and how much information of atmospheric composition one can obtain from hazy atmospheres.

There are a few theoretical studies of transmission spectra of exoplanet atmospheres that consider the effect of haze in the atmosphere (e.g., Howe & Burrows 2012; Morley et al. 2013). However, the models of haze are ad hoc; they treated the size, number density, and vertical distribution of haze particles as parameters. While they found parameter ranges in which the theoretical transmission spectra match the corresponding observations, they did not discuss if the viability of those haze properties is physically supported.

In this study, to derive realistic properties of hazes in the atmospheres of transiting exoplanets, we have developed a new theoretical model that considers the creation, collisional growth, and settling of haze particles. Also, with obtained properties of hazes, we have modeled transmission spectra of the atmospheres, using the numerical code that we developed previously. We have found that the haze particles tend to distribute in a wider region than previously thought and that haze particles of various sizes are formed in the atmosphere, which in general yield flat spectra. Simulating the transmission spectra for wide ranges of parameters concerning haze such as atmospheric composition, temperature, and UV irradiation from the host star, we constrain the parameter ranges that result in observed features in the transmission spectra. We also find the parameter ranges that show features of molecular absorptions in the spectra without being obscured by haze, making it possible to derive the information of the atmospheric composition from the observation of the transmission spectra.

Keywords: exoplanets, transits, transmission spectrum models, atmospheric composition, haze

The possibility of the homogenization of the isotopic ratio in the primordial solar nebula

TAKEISHI, Akira^{1*} ; NAKAMOTO, Taishi¹

¹Tokyo Institute of Technology

Introduction:

Star and planetary systems are formed through gravitational collapse of molecular cloud cores. Since molecular clouds consist of materials from various super novae and red giant stars, it is naturally considered that dust particles in molecular cloud cores have various isotopic ratios. On the other hand, it is known that solid materials in our solar system, especially materials of the Earth, moon, mars, and meteorites, have almost identical isotopic ratios. To homogenize isotopic ratios in solid materials, it seems that the material should be evaporated completely once, mixed well, and re-solidified. So, the homogeneous isotopic ratio in the current solar system suggests that our solar system experienced some massive evaporation events in its formation phase. However, it is not well understood which process can be responsible for such a high temperature event in the solar nebula.

Goal of this study:

We clarify if the homogenization of the isotopic ratio among all the solid materials in the solar nebula can be realized in the course of the formation and evolution of the solar nebula.

Model:

We suppose a molecular cloud core whose mass is one solar mass. The core is assumed to rotate rigidly and to consist of gas and dust particles. Dust particles have various isotopic ratios, but they are mechanically well mixed in the core. The collapse of the molecular cloud core, and the following formation and evolution of the solar nebula are modeled based on Cassen & Moosman (1981). Landing places of infalling materials from the core is estimated depending on the angular momentum. Turbulence is present in the solar nebula and the viscous torque due to the turbulence works. Also, the gravitational torque produced by the self-gravity of the solar nebula is taken into account (Nakamoto & Nakagawa 1995). The motion of dust particles relative to the gas is calculated using the turbulence diffusion model (Wherstedt & Gail 2002). The temperature of the solar nebula is obtained based on the balance between the viscous heating and the radiative cooling. The model parameters are the initial temperature and the angular velocity of the molecular cloud core. We assume that dust particles evaporate completely at the temperature of 2,000 K, and when the gas temperature becomes less than that, isotopically homogeneous dust particles are produced.

Results:

The temperature of the solar nebula becomes a decreasing function of the distance from the Sun. So, when the initial temperature of the core is high, and the initial rotation velocity of the core is low, the radius of the solar nebula becomes small and the fraction of isotopically homogeneous dust particles becomes high. For example, almost all the solid materials in the solar nebula becomes isotopically identical, when the initial temperature of the core is 15 K and the angular velocity is $(2-3) \times 10^{-14} \text{ s}^{-1}$.

Discussion:

According to observations, angular velocities of molecular cloud cores are around from 10^{-14} s^{-1} to 10^{-13} s^{-1} (Goodman et al. 1993). So, it is implied that the molecular cloud core that formed our solar system might have a smaller angular velocity compared to typical values. This may be consistent with a fact that our Sun is a single star: it is shown that molecular cloud cores having higher angular momentum tend to form binary systems, while those having lower angular momentum tend to form single star (Matsumoto & Hanawa 2003).

Conclusions:

We investigated the formation and evolution of our solar nebula following the gravitational collapse of the molecular cloud using numerical simulations. And we found that isotopic ratio of solid materials in the solar nebula can be completely homogenized, if the radius of the solar nebula is small enough due to the high temperature or the low angular velocity of the initial molecular cloud core.

Origin of the Great Red Spot and Formation of Moon and Earth's deep ocean-floor caused by Collision of mantle asteroid

TANEKO, Akira^{1*}

¹SEED SCIENCE Labo.

1. Multi-impact hypothesis: MI is a new hypothesis to the moon and the planet Earth evolution is the answer to the unified understanding of the **"Earth and Moon and Solarsystem of Mystery"**

(1). "Origin hypothesis of the moon and the deep Ocean-floor bottom by a multi-impact" was proposed a new collision mechanism to Earth's mantle piece. The differentiated Mars size of primitive planetichiusu Bourdais'law that has not been proven, was formed in the asteroid belt position.

Why was broken by perturbing tidal forces of Jupiter and flattening of the orbit of primitive planet CERRA by whether? = Jupiter perturbation **protoplanetary CERRA** was desripted.

(2). "Giant planet collision hypothesis: GI (Cameron etc.)" Problems me was discussed below.

The differentiated Mars size of primitive planet, due to the collision (**on chance of good luck**) from the revolution surface obliquely backward. = Impossible.

In hypothesis that forms the moon of only mantle component, it is not possible to explain the Earth's evolution and current status. = **Just only** a hypothesis for the origin of the moon.

2. Comparison of the two hypotheses ****MI Multi-Impact collision ****vs ****GI Giant Impact collision ****

(1). The impact velocity at the time of moon formation

****MI. (12.4km/s , 36.5 degrees) ****vs ****GI. (0~8km/s: the most die about 30 degrees) ****

(2). In Collision energy ****MI (8.01 *10³⁰J). ****vs ****GI (2.05 *10³¹J) = **about 2.56 times as MI** ****

(3). Collision probability ****New Mechanism by nature ****vs ****Non-Mechanism by Extremely small chance ****

(4). time mechanisms ******about 4 billion years ago** ****vs ******about 4.6 billion years ago** ****

3. It is possible unified understanding of **the effect of multi-impact hypothesis** ****to **"Earth and moon of mystery."** ****

(1). Whether **the five times biological large extinctions** have occurred in the earth ?

It is caused by the multiple of debris has collided to Earth.

(2).Why **large extinctions** of five degrees or more of the organism species occurs at the Earth?

Due to **the collision of the multi-impact hypothesis**.

(3). Why undifferentiated chondrite and stony achondrites, stony-iron meteorites and Iron meteorite are **mixed in the meteorite**?
The cause is the Multi-Impact the cause.

(4). Why asteroid belt was not accustomed to planet(formerly theory)?

Itokawa than crustal fragments that was differentiated?

(5). Platetectonics of **Plate boundary formation**, I suggested

"The origin hypothesis of **crust flaking** and **deep ocean-floor formation**."

(6). Why, Earthquake belt of the Pacific Rim is formed, whether the back-arc and trench has been formed?

(7). The origin of continental drift and the deep ocean floor,

I was elucidated the mystery of the driving force. **Driving force = eccentric moment of inertia**.

(8). **Why diamond pipe has been formed** in the South African Premier and Russian Mirunu'i district?

Continental drift and after collisions of Hawaii position,

collided with the opposite side of the Drake Passage of Mirunu'i mine, Antarctica is I was stabilized to move.

(9). Why earth's axis is **tilted even 23.5 degree** from the revolution surface ?

The reason for this, it was estimated that **the collision of the Drake (high latitude) CERRA division piece to the position**.

(10). **Why the Earth's core eccentricity (about 10%) has occurred?**

Earth's mantle by CERRA debris collision to the Pacific Ocean position **is missing**, is due to **Isostasy to complement it**.

(11). The new hypothesis to **the origin of the Jupiter's Great Red Spot**, Why is it ? How is it ?

***The world's first the new hypothesis ***

(12). Although other outer planets are made of gas and ice. Why Pluto is or silicate dwarf planets?

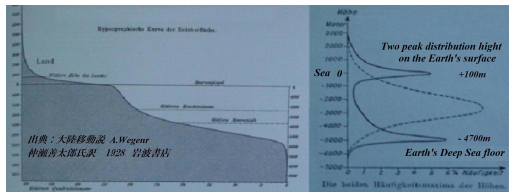
In this way, the origin of Moon and the Earth evolution according to the multi-impact hypothesis, serves the interpretation the future of **unified** understanding.

PPS21-P10

Room:Convention Hall

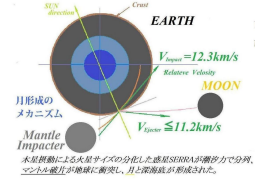
Time:May 25 18:15-19:30

Keywords: The CERRA tide division by Jupiter perturbation, Collision of the Earth, Moon formation, Formation of Earth's Deep Oceanfloor, Origin of the Great Red Spot, Origin of the asteroid belt and the meteorite



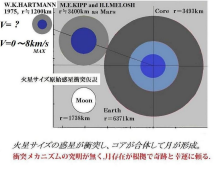
The Multi-Impact Hypothesis

[The Origin of The Moon and The Earth in Multi-Impact Hypothesis]
 Akira Iwamoto, 2014, Aug. -> 多衝突仮説による月と地球の形成



The Giant Impact Hypothesis

[Satellite-sized planetesimals and lunar origin. J. et al.
 Hartmann, W. K. and D. R. Davis 1975 Science, 24, 584-515.



A one-dimensional cloud model for Earth-like exoplanets and its stationary solution

OHNO, Kazumasa^{1*} ; OKUZUMI, Satoshi²

¹Department of Earth and Planetary Science, Graduate School of Science and Technology, Tokyo Institut, ²Graduate School of Science, Tokyo Institute of Technology

Exoplanets which have flat transmission spectrum are observed in recent years. It is thought that there are two possibility of reasons with flat spectrum. First, it is the case that the exoplanet has an atmosphere which is high average molecular mass. In this case, there are no absorption lines because atmospheres are concentrated at low levels. Second, optical thick clouds cause flat spectrum because clouds disturb starlight. It is difficult to distinguish these two cases, so it is important to predict optical properties of clouds on exoplanets.

There is a prior model of exoplanet's clouds Zsom et al.2012. This model considers microphysics of condensation, on the other hand location of cloud top and sweeping process by rain droplets are free parameters. However, this model has a problem that optical properties of clouds strongly depend on these free parameters.

The main goal of this research is to develop a self-consistent microphysical cloud model for 1D which contains not only microphysics of condensation but also microphysics of coalescence by cloud droplets and rain droplets. We present a self-consistent microphysical cloud model for 1D atmosphere calculating revolution of cloud droplets and rain droplets to consider coalescence process. Furthermore, our cloud model introduces a physical parameter which is updraft velocity, on the other hand location of cloud top and sweeping process by rain droplets are automatically determined.

We apply this model to Earth and obtain the following results. Quiet atmospheres (updraft velocity is less than 0.1m/s) and clean atmospheres (number density of cloud condensation nuclei is less than 10cm^{-3}) can make optical thin cloud. These results are caused by decreasing cloud droplets by downturn of cloud top, coalescence process and sweeping process by rain droplets. Furthermore, we reveal that rain droplets sweep 70% cloud droplets. These results which argue the possibility of forming optical thin clouds on exoplanets are new results which we can get by considering location of cloud top and coalescence process.

Our cloud model enables to determine the vertical distribution and optical properties of exoplanetary clouds as a function of physical atmospheric parameters. The development of this research is to estimate an impact of exoplanet's cloud on transmission spectrum.

Semi-analytical estimation of the ocean tide on the early Earth

MOTOYAMA, Mai^{1*}; TSUNAKAWA, Hideo¹; TAKAHASHI, Futoshi²

¹Department of Earth and Planetary Sciences, Tokyo Institute of Technology, ²Faculty of Sciences, Kyushu University

We have investigated the ocean tide on the early Earth using semi-analytical method. The tidal force of the Moon exerted on the Earth is considered to have been an order of magnitude larger at the early time than at present, since the Earth-Moon distance was smaller (Goldreich, 1966). Abe et al (1997) and Abe and Ooe (2001) performed numerical simulation of the early Earth's ocean tide, estimating amplitudes of ~ 0.1 m for three uniform depths of the ocean (1000 m, 2600 m and 4200 m). They pointed out that such small amplitudes are caused by the difference of periods between the early Earth's rotation and the free oscillation of the ocean. This result is important to study the ancient surface environment on the Earth. However the accurate ocean depth on the early Earth has not been established yet, although it could be several times as large as the current. The free oscillation of a thin layer of the ocean with a certain constant depth over the Earth can be described with Laplace's tidal equations. Longuet-Higgins (1968) numerically solved the Laplace's tidal equations, showing the relation between the eigenfrequency and Lamb's parameter. Based on his results, we have derived semi-analytical expression for the relationship between the ocean depth and the Earth's rotation period as possible resonance of various oscillation modes. If the Earth's angular velocity have changed in a range of 1 — 4.8 times relative to the present value, the ocean depth for the resonance is estimated to be 17 — 420 km for P_2^2 mode, 0.5 — 13 km for P_3^1 mode, and 18 — 480 km for P_3^3 mode. These results indicate that semidiurnal mode (P_2^2) would have been very small as shown by previous studies, unless depth of the early ocean was more than six times greater than the current. However P_3^1 mode could be larger than P_2^2 mode due to resonance during the orbital evolution of the Moon, although the amplitude depends on attenuation due to eddy viscosity of the ocean.

Keywords: Ocean tide, Dynamical evolution of earth-moon system, primitive Earth, eigenfrequency, eigenfunction, tidal force

The attenuation behavior of shockwaves induced by hypervelocity impacts investigated using the iSALE shock physics code

KUROSAWA, Kosuke^{1*} ; KAMATA, Shunichi²

¹PERC/chitech, ²Graduate School of Science, Hokkaido University

The dominant geographical features on airless planets and/or satellites are impact craters. Such craters are an evidence that planets and satellites suffered a numerous number of hypervelocity impacts during their histories. The kinetic energy of an impactor is transferred into a target body as a strong shockwave, leading to phase changes, including vaporization, melting, and the transition into a high-pressure phase, and characteristic feature by fracture, i.e., shutter cones. Quenched high-pressure minerals and the impact-induced geological features in strata on the Earth provide us useful information to investigate the surface history of the Earth. Recently, such high-pressure minerals have found from the Apollo rock samples and meteorites by new techniques for analyses. A physical model, which describes shockwave attenuation after a hypervelocity impact under a wide range of impact conditions, is necessary to investigate the impact history on such small bodies based on such shock indicators. However, the impact outcomes on such small bodies have not been fully understood because the effects of surface gravity, porosity, strength, and temperature profile on the shock propagation into a target body have not been studied well.

In this study, we conducted a series of numerical calculations using the iSALE shock physics code to investigate the shock attenuation under a various impact conditions. We are able to numerically solve the attenuation behavior of an impact-generated shockwave due to an interaction between the shockwave and a rarefaction wave from a free surface by using the iSALE. In addition, iSALE includes various material models, including granular materials, rocks, and metals, and a porosity compaction model. Thus, iSALE is highly suitable for our purpose. We obtained preliminary results as described following; (1) the target porosity significantly enhances the degree of the shock attenuation, (2) the degree of the shock attenuation for visco-elast-plastic bodies is larger than that for an inviscid fluid, (3) the internal friction of the target material changes the wave profile of the shockwave, (4) a higher target temperature leads to a higher degree of the shock attenuation. We are planning to construct the physical model based on a number of numerical results under a wide range of impact conditions.

We gratefully acknowledge the developers of iSALE, including Gareth Collins, Kai W̄nnemann, Boris Ivanov, Jay Melosh, and Dirk Elbeshausen.

Keywords: Hypervelocity impacts, Shock propagation, High-pressure minerals, Shutter cones, Shock physics code

Development of Compressible and Non-Expanding Fluid Solver for Simulation of Impact and Penetration Dynamics

SUZUKI, Kojiro^{1*}

¹GSFS, The University of Tokyo

An impact probe called penetrator is expected to play an important role in the exploration of the interior of an object in the solar system, especially at a low-cost small mission. To realize the penetrator mission, the analysis model of the penetration dynamics must be established. The fact that the force model based on the Newtonian theory for the aerodynamic prediction of hypersonic flying objects is still effective not only for a penetrator into the regolith (Suzuki, et al., 20th ISTS, 96-i-02V, 1996) but also for that into ice (Suzuki, et al., 30th ISTS, 2015, to be presented) implies that the motion of soil particles or fragmented ice pieces can be macroscopically described in a framework of fluid dynamics. Unlike well-known compressible gas, expansion does not occur at unloaded state or exposure to the vacuum. In the present study, for the purpose of the numerical simulation of impact and penetration dynamics, we consider the compressible but non-expanding fluid (hereinafter referred to as CNEF) model, and the Riemann solver is developed for it.

For the numerical analysis of impact problems, the SPH (Smoothed Particle Hydrodynamics) method is often used with some appropriate fluid dynamics model. Though numerical instability of the SPH method can be overcome by applying Godunov scheme (Namba, et al., CFD symposium, D02-2, 2014), particle-based methods still have problems in computational efficiency and description of rigid surfaces. Consequently, we use the finite volume method with the Godunov scheme for numerical simulation of CNEF flows.

To avoid the appearance of expansion waves in a CNEF flow, we assume that the pressure increases with the density only at loading and it instantaneously becomes zero without changing the density at unloading. By using such pressure model, the CNEF only allows the formation of shock waves. Expansion waves are not formed at all. Instead, it allows for the void (or vacuum) to be formed in a flow. Neglecting the effects of viscosity and diffusivity for simplicity of analysis, the dynamics of a CNEF flow is described by the inviscid Euler equations combined with the above pressure model. It should be noted that the pressure is not a quantity of state any more, because it depends on the path of the process. To consider the presence of a void in a flow, the VOF method (Hirt, C. W. and Nichols, B. D., J. Comp. Phys., 39, 1981) is used.

For the numerical simulation of a CNEF flow with the finite volume method and the Godunov scheme, the Riemann solver is necessary. At present, we have found four types of the fundamental solutions: a) translational motion of the fluid in vacuum, b) a pair of running shock waves formed at the collision between two lumps of fluid, c) formation of unloaded zone at a rear-end collision, and d) separation between a quicker front runner and a slower second runner. We have analytically obtained the fundamental solutions assuming that the pressure linearly increases with the density at loading. The numerical results for the test problems on the one-dimensional collision show that after the collision, two lumps of fluid are combined into a single lump without formation of expansion waves as expected for the CNEF model. For the future works, all the fundamental solutions for the Riemann problem of CNEF should be mathematically confirmed, and the CNEF model should be improved to be suitable for actual impact dynamics problems.

This work is supported by Grant-in-Aid for Scientific Research (B) No. 25289301 of Japan Society for the Promotion of Science.

Keywords: impact, numerical simulation, fluid dynamics, Riemann solver

1-D Plane Parallel Shock Waves of Dust-Gas Mixed Fluid: For Simulations of Chondrule Forming Planetesimal Bow Shocks

KATSUDA, Yuya^{1*} ; NAKAMOTO, Taishi¹

¹Tokyo Institute of Technology

Chondrules are millimeter sized silicate composition spheres that are the dominant component in most chondritic meteorites. It is considered from experiments and measurements that chondrules experienced flash heating events and melting/re-solidification in the early solar nebula. The shock wave heating model is one of the most viable models for chondrule formation. And we think that eccentric planetesimals are the source of shock waves in the solar nebula.

Planetesimal bow shocks for chondrule formation have been studied by some work (e.g., Boley et al. 2013, Ciesla et al. 2004). In those works, the dust-to-gas mass ratio was considered to be around the standard solar value, which is about 1:100. On the other hand, based on petrological studies, it is considered that the partial pressure of oxygen in the gas around the molten chondrules was considerably higher than the canonical value. If the oxygen in the gas is supplied from evaporated dust particles, the initial dust-to-gas mass ratio is estimated to be 1:1 or 10:1 (Jones et al. 2000). When the dust-to-gas mass ratio in the fluid is high enough, physical and chemical effects of dust on the flow would not be negligible. So, in order to investigate the chondrule formation by shock waves in the dusty condition, we need to carry out hydrodynamical simulations with high dust/gas mass ratio.

In this study, first, we examine 1-D plane parallel shock waves of dust/gas mixed fluid with high dust/gas mass ratio. Especially, we clarify a relation between physical quantities behind the shock waves and the dust/gas mass ratio. Then, for our future study, we develop a numerical code to simulate the dust rich fluid. We assume that the size of dust particles is small enough so the motion and the temperature of dust particles are the same with those of the gas. We also assume that the dust particles evaporate completely when their temperature exceeds 2,000 K.

First, we analytically obtain the relation of the temperature, density, velocity, and the pressure between before and behind the shock wave, when the energy transfer is not taken into consideration (adiabatic case). When the dust particle is not incorporated in the fluid at all, this relation is known as the Rankine-Hugoniot relation. And we extend the relation so that the effects of dust particles are taken into account. According to the relation obtained here, we found that the density, pressure, and the velocity behind the shock do not depend on the dust/gas mass ratio, the temperature rises as the dust/gas mass ratio increases. These dependences can be understood based on the mass and the momentum conservation. The temperature behind the shock is an increasing function of the dust/gas mass ratio, because the gas number density behind the shock becomes lower as the dust/gas mass ratio increases, but the pressure should be the same, so the temperature should be higher.

Second, we carried out numerical simulations of 1-D plane parallel shock waves using the numerical code developed for this study. We found that numerical results are in a good agreement with analytical solutions. Thus, we think that the developed numerical code is applicable for future simulations that include 2-D geometry and radiative energy transfer.

Keywords: chondrule, shock wave, hydrodynamics simulation

A numerical simulation on diurnal thermal waves of an asteroid surface with detailed topographical model

TAKITA, Jun^{1*} ; TANAKA, Satoshi² ; SENSHU, Hiroki³

¹Graduate School of Science, Tokyo University, ²ISAS/JAXA, ³Planetary Exploration Research Center, Chiba Institute of Technology

The numerical-shape model of asteroid Itokawa is available to perform the combined calculation of thermo physical state of a planetary surface in surface topography and thermal inertia. The spatial resolution of numerical shape model for a thermal observation in a future exploration will require the appropriate scale of the surface topography to explain the observed data in physically meaningful manner, which will determine the issue of understanding of the thermo physical state of asteroids. The thermo physical modelings for spherical planet including lunar and mercury are successful for explaining observational results with spatial resolutions. However the classical thermal models for ground based observation to explain the light curve of point of light asteroid fails to explain the spatially-resolved monitoring images that contains the distribution of surface temperature in thermal infrared wave length. The new thermo physical modeling style needs constructing to adequately simulate the thermal state of a planet with specially resolved none-spherical topographical perspective. The thermal state of NEA is explained in black body approximation in terms of albedo and thermal emissivity. The additional features will be expected when we consider the topographical effect in thermo physical modeling of an asteroid, which contains self-shadowing effect, thermal re-radiation heating and scattering of direct solar flux of the surface. When we take the black body approximation into account, the former two effects becomes more important to calculate the temperature of an asteroid with spatially-resolved numerical shape models which will be different from spherical models with no such secondary effects.

The thermo physical state of an asteroid surface is well described in thermal inertia of surface materials of the planet. The degree of thermal inertia can be estimated by reproducing diurnal thermal profiles of surface temperature, whose difference from spherical thermal models is necessary to be evaluated as well as the accuracy and feasibility of the estimation. The accuracy depends upon imaging frequency of an on-board imaging device, which in turn is supposed to be used for the purpose of deciding the imaging operation for investigating the accuracies of thermal inertia, conversely. The effect of local topography (several m) as well as the global shape (several hundred m) is considered at the same time in this study.

Keywords: asteroid, surface temperature, spatial resolution, thermal modeling, topography, thermal inertia

Thermal evolution simulation of asteroid Vesta

NOGAMI, Tatsuhiko^{1*} ; SHIRONO, Sin-iti¹

¹Division of earth and planetary science, Nagoya university, ²Division of earth and planetary science, Nagoya university

Vesta has been regarded as the parent body of the HED meteorites. From the observation of DAWN spacecraft, the uppermost layer of Vesta is composed from howardite ranging from 50km to 80km (Jutzi et al. 2013). It is known that the ratio of the number of eucrites to diogenites is around two. Based on these facts, rapidly cooled magma layer on Vesta should be more than 10km in thickness.

In this work, I studied the evolution of internal thermal evolution of Vesta due to heating of decay of ²⁶Al. I calculate the temperature distribution by solving numerically heat conduction equation. According to Formisano et al.(2013), if Vesta completed its formation within 1.4Ma from the injections of ²⁶Al into the solar nebula, the degree of silicate melting of inside Vesta exceeds 50 vol%. But in that work, convection and melt migration were not taken into account. These two mechanisms contribute to cool Vesta. So it is expected that the formation of Vesta is completed more early if these are taken into account. By the way, it is known that it takes about a few hundreds year for Vesta-size planet to complete its formation in planetary formation standard model.

As a convection model, I adopted the simple model of Kaula (1979). It was assumed that generated melt migrates the surface instantaneously, and the migrating melt to the surface was accounted as the rapidly cooled magma. There are two parameters in this study, including a (the percentage of melt migration) and t₀ (formation time of Vesta), and perform simulation taking into account the convection and melt migration.

As a result, convection and melt migration substantially change the evolution of internal thermal structure, and total eruptive volume of melt considerably depends on a and t₀. The magma volume increases as a increases. On the other hand, the magma volume decreases as t₀ increases.

When t₀=0, corresponding to no decay of ²⁶Al at the beginning, and a>0.3, the erupting magma layer of 10km in thickness is formed. When a=1, that is all melt is erupted, the erupting magma layer of 10km is formed if t₀<0.9Ma. According to these results, Vesta should be completed its formation within 0.9Ma after CAI formation, and more than 30% of generated melt should migrate the surface. But all generated melts aren't necessarily erupted, and if a<1, Vesta has to be completed more early.

Therefore, it is suggested that the formation time of Vesta should be more early than the estimate by Formisano et al.(2013), and that planetary formation standard model might have to be reviewed.

Jovian core formation at the boundaries of dead zone: dependence on the gas surface density distribution

SIRONO, Sin-iti^{1*} ; KATAYAMA, Masahumi¹

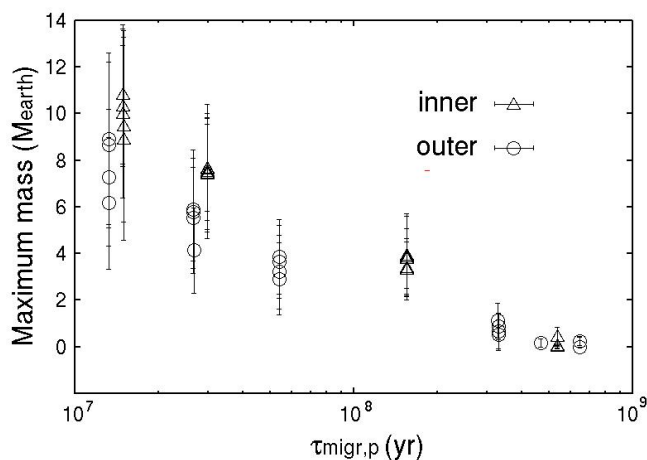
¹Graduate School of Environmental Sciences, Nagoya University

In a protoplanetary nebula, dead zone is formed where the viscosity is low because of low ionization fraction. There is a large variation in viscosity at the boundary of dead zone. This variation leads to the formation of vortices which can trap dust aggregates. A protoplanet can be formed in short timescales in a vortex. Sandor et al. (2011) showed that a core of Jovian planet is formed within a few Myr at the boundaries of dead zone.

In this simulation, a gas surface density distribution obtained from Lyla et al.(2009) is adopted. We changed the heights of two peaks in the distribution and checked the dependence of the largest mass on the height. We confirmed that the migration timescale of a planet inversely proportional to the peak height. It has been shown that the largest mass depends on the migration timescale logarithmically. This result indicates that the time evolution of the gas surface density cannot be neglected in the formation of a core. We will present the simulation results taking account of the time evolution of gas surface density distribution.

Fig 1: Maximum mass at the inner (triangles) and outer (circles) boundary of dead zone. Error bars show the standard deviation for 100 simulation runs.

Keywords: jovian planet, core, dead zone, gas surface density distribution



Measurements of the density, permittivity, and crack distribution in basalt targets based on the impact experiment

ISHIYAMA, Ken^{1*} ; KUMAMOTO, Atsushi¹ ; TAKAGI, Yasuhiko² ; NAKAMURA, Norihiro³ ; HASEGAWA, Sunao⁴

¹Department of Geophysics, Tohoku University, ²Department of Regional Business, Aichi Toho University, ³Department of Earth Science, Tohoku University, ⁴ISAS/JAXA

The many meteorites have impacted the lunar surface during ~ 4.6 Ga, in which the crater terrain is formed. In lunar nearside, the lunar lava (basalt) covers the inside of the basins (mare region), formed by large meteorites. The Lunar radar sounder (LRS) onboard the Japanese lunar orbiter SELENE (KAGUYA) radiated the electromagnetic wave in the Moon and succeeded in detecting the lunar surface and subsurface reflectors in the mare region [Ono et al., 2009]. Using the LRS data, Ishiyama et al. [2013] estimated the bulk permittivity of the lunar uppermost basalt layer and suggested a high porosity (more than $\sim 20\%$) of mare basalts. This estimated porosity is higher than the porosity of the Apollo basalt samples, so that the impact-induced macro cracks, which are not included in the Apollo basalt samples, are probably introduced in the lunar uppermost basalt layer. However, we cannot evaluate the subsurface distribution of the impact-induced macro cracks and the effect of the cracks on the permittivity estimated from the LRS data. Therefore, we produce the artificial impact crater on the basalt target based on the impact experiment, and measure the density, permittivity, and crack distribution in the basalt target.

We performed the impact experiment by using the two-stage light-gas (hydrogen) gun at JAXA on December 2014. The spherical stainless projectiles (0.32 cm in diameter and 0.133 g in mass) were launched at the velocities of 3.5, 4.5, 5.5, 6.5 km/s to investigate the impact velocity dependency and impacted on the basalt targets of 20 cm \times 20 cm \times 10 cm. We repeated the impact experiment twice for each impact velocity in order to confirm the repeatability. Next, we drilled core samples (2.5 cm in diameter and 8-10 cm in length) from the basalt targets along a horizontal and depth directions in order to investigate the effect of anisotropic crack on the permittivity. This investigation gives us the opportunity of the verification based on the effective medium theory [e.g., Sihvola, 1988], which supposes the effect of anisotropic crack on the permittivity. Finally, we sliced the core sample each of ~ 4 mm in thickness and polished the surface of sliced samples to measure permittivity and surface crack distribution.

We estimated the density of the sliced sample from the measurements of its mass and volume, and investigated the crack fraction by scanning the surface of the sliced thick sample. The permittivity of the sliced thick sample was measured at 5 MHz by using the permittivity measurement system (TOYO Technica Corporation: Type-1260 impedance analyzer and Type-12962A interface) for measuring the permittivity. In the presentation, we will report the initial analysis result of the sliced samples.

Acknowledgement: This study was supported by ISAS/JAXA as a collaborative program with the Space Plasma Laboratory.

Structure of the accretion disk around a protostar and the planetesimal formation (II)

IMAEDA, Yusuke^{1*} ; EBISUZAKI, Toshikazu¹

¹RIKEN

We constructed steady-state protoplanetary disk models that can explain the local concentration of the solid materials in the disk. The enhancement of the particle to gas ratio in the disk is favorable for the planetesimal formation scenario through the gravitational instability (Youdin and Shu 2002).

We considered one dimensional viscous accretion disk in steady-state as the disk model. The disk structure is determined by the balance of the angular momentum flux and the viscous torque, the balance of the viscous heating, the irradiative heating, and the radiative cooling as the function of mass accretion rate. The viscous process is determined by the Magnetorotational Instability (MRI). Whether MRI is active or inactive is determined by the ionization degree. In addition to the galactic cosmic rays and the radioactive nuclei, we take into account the thermal ionization as the ionization source in this study, which brings the inner disk becomes MRI active. The previous works (Balbus and Hawley 2000) showed that this thermal ionization boundary was located very close to the central star (0.1AU or less). We, however, found that the viscous heating of the disk sifts the front location outward to nearly 1 AU for the case of mass accretion rate, 10^{-7} Ms/yr.

In this transition region (inner MRI front), the drift velocity of the solid particles turns out to be outward because of the positive pressure gradient at the mid-plane of the disk. This change in drift direction leads the concentration of solid particles around the boundary. Since the drift velocity is size dependent, this concentration mechanism is also size dependent. Small particles larger than 1cm can be trapped, but less than 1mm pass this front. The temperature of this region is around 1000K-1300K. The planetesimals are likely to be almost volatile free, if they formed in such a high temperature. We discuss our disk model and the implications to the planetesimal formation and the chemical compositions of meteorites in more detail in the presentation.

Keywords: protoplanetary disk, planetesimal formation, magnetorotational instability

The effect of the condensation of ice components on the theoretical estimate of the thermal evolution of ice giants

KUROSAKI, Kenji^{1*} ; IKOMA, Masahiro¹

¹Department of Earth and Planetary Science, The University of Tokyo

Though Uranus and Neptune are similar in mass and radius, the former is significantly fainter than the latter. Most of previous theoretical studies of thermal evolution of ice giants assumed three-layer models composed of a hydrogen-helium envelope, an ice mantle and a rocky core. According to them, the observed effective temperature of Uranus is lower than theoretically predicted (e.g., Fortney et al., 2011; Nettelmann et al., 2013). Previous studies did not consider the condensation of ice components in the atmosphere.

The difference between Uranus and Neptune might be whether they experienced a giant impact event or not. Uranus is believed to have experienced a giant impact, since the axis of rotation of Uranus is tilted to the orbital plane (Slattery et al., 1992). The giant impact may have mixed Uranus's hydrogen and helium in the envelope with ice components and the planet has a significant amount of ice components in its atmosphere. If this is true, the initial compositional distribution is expected to be different between Uranus and Neptune. Especially, the effect of condensation is not negligible for Uranus.

In this study, we consider the thermal evolution of ice giants considering the condensation of ice components in the atmosphere. During the thermal cooling of the planet, the ice components in the atmosphere condense and then moist convection occurs. Then, the cooling of the planet is controlled by the radiation limit. The radiation limit appears when the optical depth and temperature structure of the entire atmosphere approach a fixed profile. Consequently, the effect of the condensation makes short the timescale of the thermal evolution of the planet. That effect is important to understand the difference of the thermal evolution between Uranus and Neptune.

Keywords: ice giants, thermal evolution